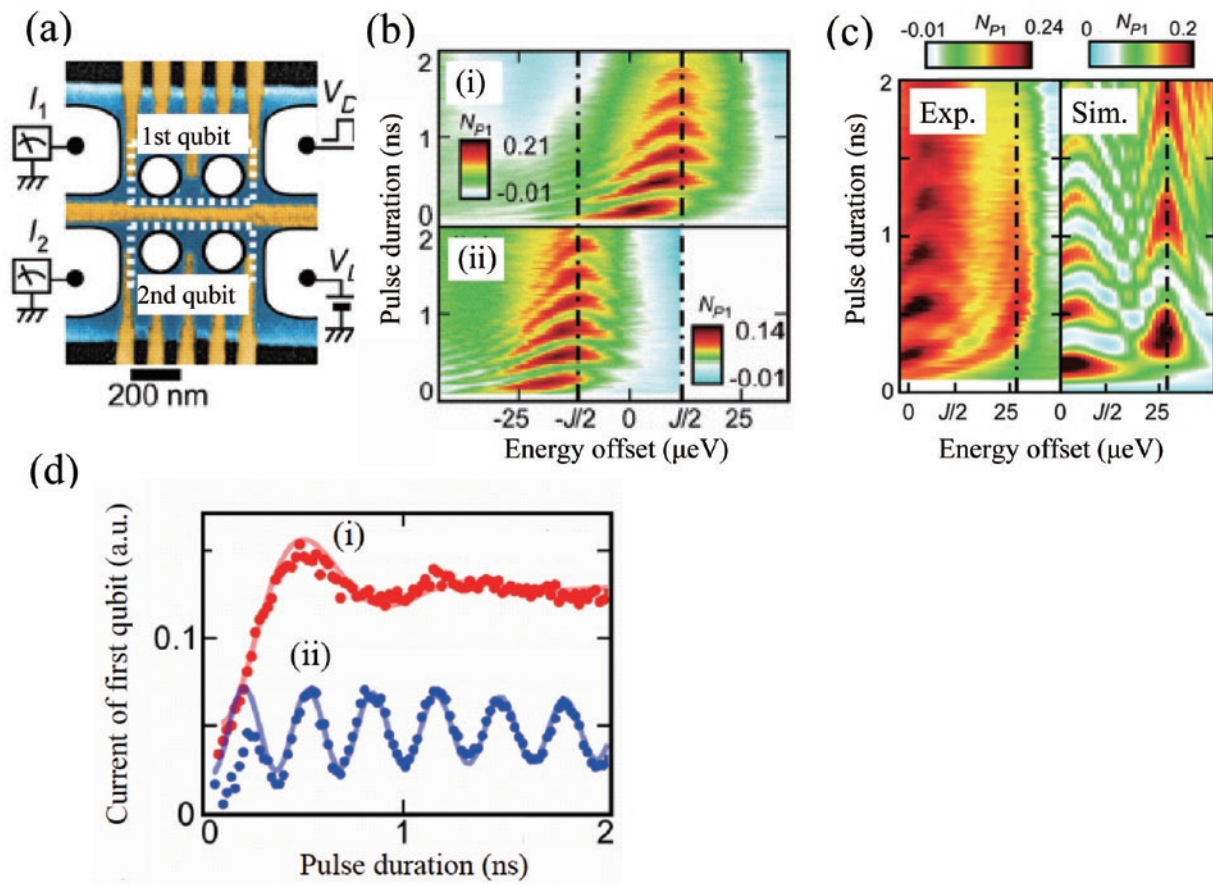


Research Activities in NTT Basic Research Laboratories

Volume 20
Fiscal 2009

July 2010

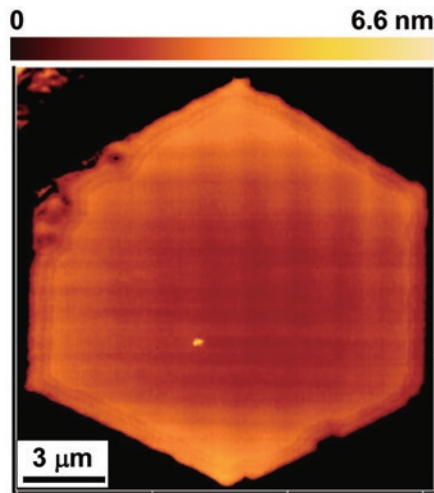
NTT Basic Research Laboratories,
Nippon Telegraph and Telephone Corporation (NTT)
<http://www.brl.ntt.co.jp/>



Cover photograph:

Multiple Two-qubit Operations Using Semiconductor Coupled Charge Qubits

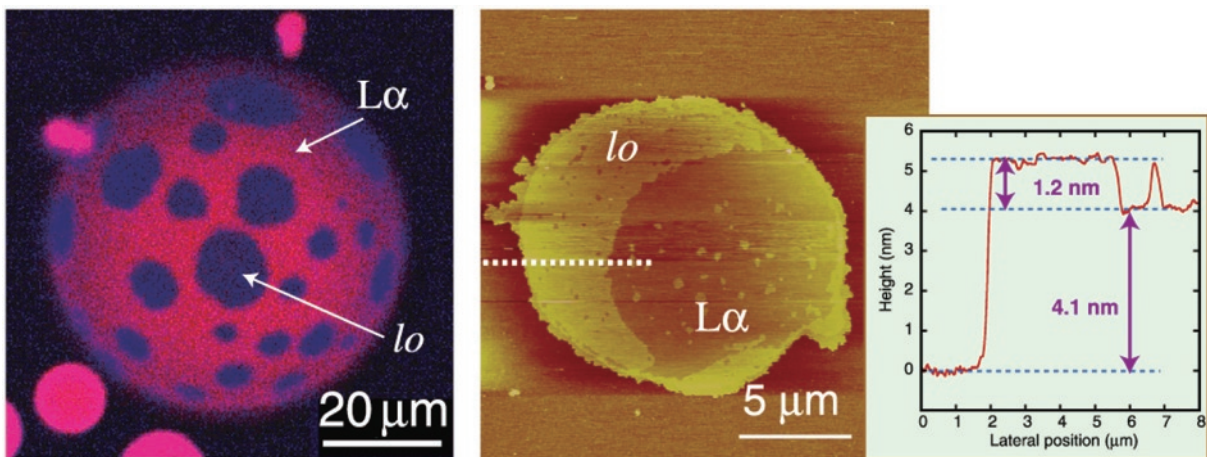
Two-qubit unitary operations such as controlled rotation (CROT), which rotates the target qubit state conditionally on the control qubit state, and SWAP, which swaps quantum states of the two qubits, are important for performing quantum algorithms and correlating multiple qubits. Using coupled semiconductor charge qubits consisting of two pairs of double quantum dots (DQD), we demonstrated CROT and SWAP, each in a single step. (a) Scanning electron micrograph of the two-qubit device. (b) Coherent oscillations of the first qubit representing the CROT operation. Oscillations (i) and (ii) correspond to cases where the second qubit is in states $|1\rangle$ and $|0\rangle$, respectively. (c) Data showing additional slow oscillations along the dot-dash line corresponding to correlated coherent oscillations of the first qubit. (d) Correlated coherent oscillations of the first qubit (i). This corresponds to the data along dot-dash line in (c). Oscillation (ii) corresponds to the conditional coherent oscillations along the dot-dash line in (b). (Page 31)



Photograph of atomic force microscopy

Step-free GaN Surfaces Fabricated by Selective-area Metalorganic Vapor Phase Epitaxy

A step-free GaN surface with the diameter of 16 μm , which was atomically flat without any monolayer steps, was fabricated for the first time by selective area metalorganic vapor phase epitaxy. This technique can control the hetero-interfaces of nitride semiconductors in an atomic scale and realize high-efficiency light emitting devices and sabband devices, such as resonant tunneling diodes and cascade lasers. In addition, we clearly observed the nucleus growth of nitride semiconductors and investigate the mechanism in detail. (Page 16)

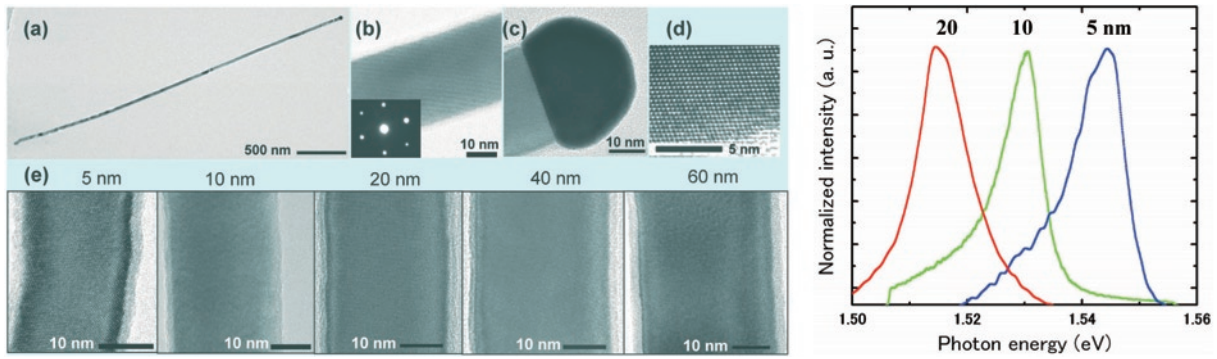


Liquid ordered domains on a GUV (fluorescent image).

AFM image and line profile of the domains on a supported lipid bilayer after the GUV rupture.

Formation of Liquid-ordered Domains on a Giant Unilamellar Vesicle

Liquid-ordered (*lo*) domains (raft-like domains), play an important role in regards to the function and arrangement of membrane proteins. Here, we form *lo* domains on a giant unilamellar vesicle (GUV). The GUV can be ruptured by increasing the salt concentration in the buffer solution and screening the repulsive electrostatic interaction between the GUV and the substrate. These micron-scale domains on a supported lipid bilayer will help to control membrane proteins in nano-bio devices. (Page 23)

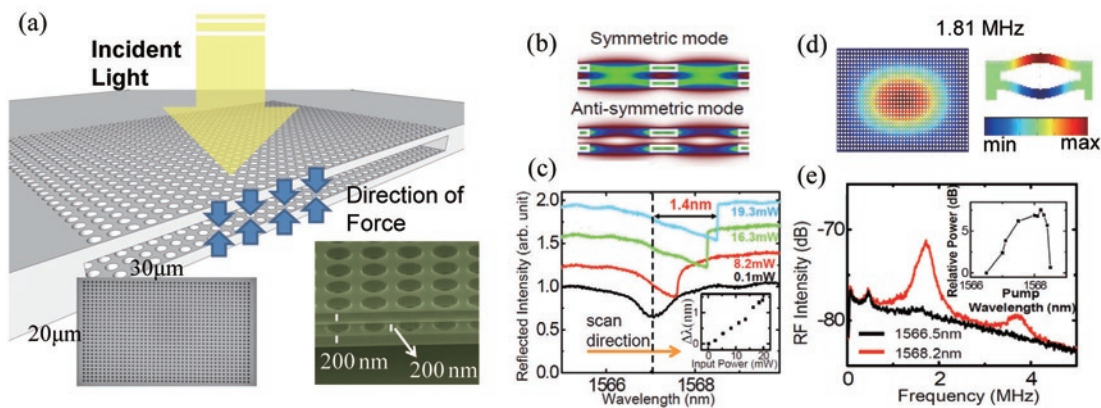


Transmission electron microscope (TEM) images of free standing GaAs nanowires (NWs). (a) single NW. (b) and (c) High-magnification images (d) HRTEM image near the NW side. (e) images for Au particles with different diameters.

Photoluminescence spectra for GaAs NWs grown using Au particles with three nominal diameters.

Freestanding GaAs Nanowires with the Controlled Diameter and Their Optical Properties with the Radial Quantum-confinement Effect

Semiconductor nanowires (NWs) have attracted considerable attention due to the interesting fundamental properties of such low-dimensional systems. With a view to exploring the potentially unique applications of the freestanding-type nanowires, we synthesized freestanding GaAs NWs with a controlled diameter using size-selective Au particles via the Au-catalyzed vapor-liquid-solid method, and successfully observed the luminescence blue shift induced by the radial quantum-confinement effect. Our work opens the way to investigating size-related optical phenomena in bare GaAs quantum wires, and provides more opportunities for the study of one-dimensional quantum physics using freestanding NWs. (Page 39)



(a) Schematic and SEM images of bi-layer PhC (Force for symmetric mode is depicted). (b) photonic bandedge modes in the bi-layer PhC. (c) power dependence of reflectance spectra for the symmetric mode. (d) fundamental vibration mode with odd symmetry to modulate optical mode. (e) RF spectra of reflected light.

Ultralarge Optomechanical Coupling in a Bi-layer Photonic Crystal

We realized bi-layer photonic crystal (PhC) embedding a thin air gap and observed its optomechanical coupling phenomena. Two InP PhC slabs with thickness of 200 nm were separated by an air gap with thickness of 200 nm. We could observe large shift of bandedge mode in reflectance spectra. This can be explained by displacement of the PhC slabs by huge radiation force, resulting from strong optomechanical coupling. Such strong optomechanical coupling also allowed the tiny Brownian motion of slabs to modulate optical resonant mode, which could be observed as a peak in the RF spectra of the reflected light beam. (Page 42)

Message from the Director



We are extremely grateful for your interest and support with respect to our research activities.

The three research areas at NTT-BRL, namely Materials Science, Physical Science, and Optical Science, are undertaking work designed to create new values supporting NTT's future business and to promote advances in science that will ultimately benefit all mankind.

A fundamental goal of these research activities is to improve global competitiveness. Therefore, BRL is collaborating with many universities and research institutes throughout the world as well as with other NTT laboratories. BRL organizes international conferences related to quantum physics and nanotechnology and also holds a "Science Plaza" to enhance public understanding of our activities and to ensure a frank exchange of opinions. Moreover,

one of our missions is the education of young researchers and we sponsor the biennial "BRL School", which boasts distinguished researchers as lecturers. In November 2009, thirty-five Ph.D. students and young researchers from universities and institutes in 9 countries participated in the BRL School. We hope that this endeavor will encourage research and contribute to its future growth.

It gives us immense pleasure to fulfill our mission of being an open laboratory, and to disseminate our research output worldwide. Your continued support is greatly appreciated.

A handwritten signature in cursive script that reads "Itaru Yokohama".

Itaru Yokohama
Director
NTT Basic Research Laboratories

Contents

page

◆ Cover	
◆ Multiple Two-qubit Operations Using Semiconductor Coupled Charge Qubits	
◆ Color Frontispiece	I
◆ Step-free GaN Surfaces Fabricated by Selective-area Metalorganic Vapor Phase Epitaxy	
◆ Formation of Liquid-ordered Domains on a Giant Unilamellar Vesicle	
◆ Freestanding GaAs Nanowires with the Controlled Diameter and Their Optical Properties with the Radial Quantum-confinement Effect	
◆ Ultralarge Optomechanical Coupling in a Bi-layer Photonic Crystal	
◆ Message from the Director	III
◆ NTT Basic Research Laboratories Organogram	1
◆ Member List	2

I. Research Topics

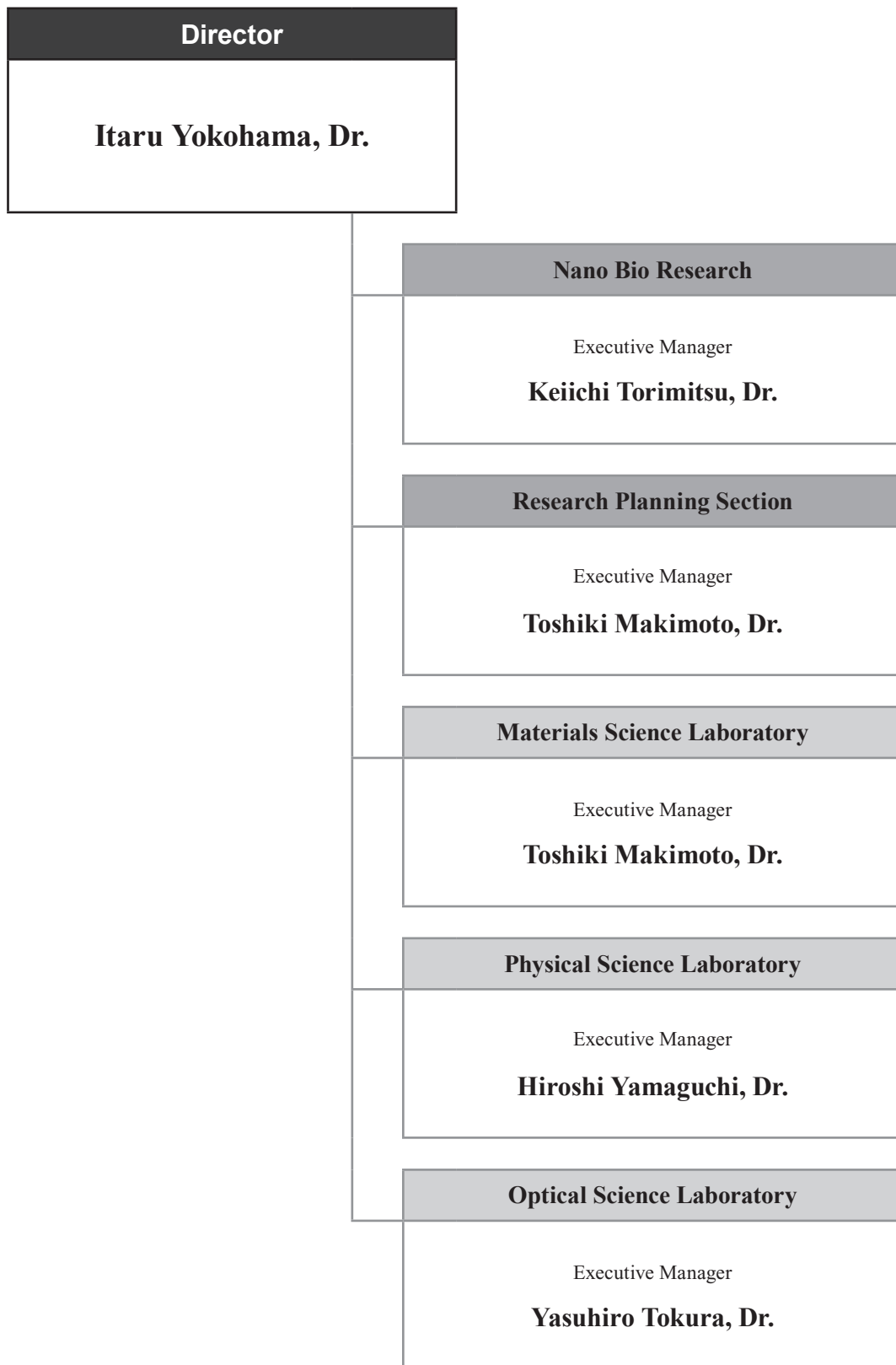
◇ Overview of Research in Laboratories	13
◇ Materials Science Laboratory	14
◆ Improvement of H-terminated Diamond FETs in NO ₂ Atmosphere	
◆ Single-crystal AlN (0001)/diamond (111) Heterostructure	
◆ Step-free GaN films Grown by Selective-area Metalorganic Vapor Phase Epitaxy	
◆ Synthesis of the Parent Compound Superconductors RE ₂ CuO ₄ by MBE and Specially-designed Post-reduction	
◆ Growth of Graphene by Gas-source Molecular Beam Epitaxy	
◆ Stability-instability Transition of Reaction Fronts in Thermal Silicon Oxidation	
◆ Stacking Domains in Epitaxial Bilayer Graphene	
◆ Carbon Nanotube Synthesis from Diamond	
◆ Effect of Mg ²⁺ on Neural Activity	
◆ Fabrication of a Nano-bio Device Using Giant Unilamellar Vesicles	
◆ Design of an LSI Chip for a Bio-machine Interface in 0.18 μm CMOS Technology	
◇ Physical Science Laboratory	25
◆ Si Nanowire Ion-sensitive Field-effect Transistors with a Shared Floating Gate	
◆ Tunneling Spectroscopy of Electron Subbands in Thin SOI-MOSFETs	
◆ Two-dimensional Patterning by Using Block Copolymer Self-assembly	

◆ Optical Tuning of Coupled Nanomechanical Resonators	
◆ Intrinsic Gap and Exciton Condensation in the $\nu_T = 1$ Bilayer System	
◆ Fano-Kondo Effect in a Side-coupled Double Quantum Dot	
◆ Multiple Two-qubit Operations Using Semiconductor Coupled Charge Qubits	
◆ Theory of Quantum Dynamics During a Qubit Readout Process with a Josephson Bifurcation Amplifier	
◆ Experimentally Realizable Controlled-NOT Gate in a Flux-qubit / Resonator System	
◆ Kondo Effect in a Semiconductor Quantum Dot Controlled by Spin Accumulation	
◇ Optical Science Laboratory	35
◆ Generation of Time-bin Entangled Photon Pairs Using Cascaded Second Order Nonlinearity in Single PPLN Waveguide	
◆ Numerical Analysis of Cold Fermionic Atoms in an Optical Lattice at Finite Temperatures	
◆ Trapping Loss Mechanism of Superconducting Atom Chips	
◆ Ultrafast Dynamics of Coherent Phonons in P-type Si Driven by Sub-10-fs Laser Pulses	
◆ Freestanding GaAs Nanowires with a Controlled Diameter and Their Optical Properties with the Radial Quantum-confinement Effect	
◆ Photoluminescence Properties of Dynamic Quantum Dots Formed by Surface Acoustic Waves	
◆ Sub-femtojoule All-optical Switching Using a Photonic Crystal Nanocavity	
◆ Strong Optomechanical Coupling in a Bi-layer Photonic Crystal	
◆ All-silicon Photonic Crystal Receiver for 1.55- μm Light Detection Utilizing Two Photon Absorption	

II. Data

◇ Science Plaza 2009	45
◇ 5th NTT-BRL School	46
◇ Award Winners' List	47
◇ In-house Award Winners' List	48
◇ Research Activities in Basic Research Laboratories in 2009	49
◇ List of Invited Talks at International Conferences	51

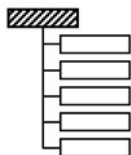
NTT Basic Research Laboratories Organogram



Member List

As of March 31, 2010
(* / left NTT BRL in the middle of the year)

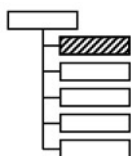
NTT Basic Research Laboratories



Director, **Dr. Itaru Yokohama**

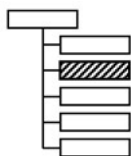
Dr. Junji Yumoto*

Nano Bio Research



Executive Manager, **Dr. Keiichi Torimitsu**

Research Planning Section



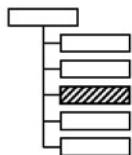
Executive Research Scientist, **Dr. Toshiki Makimoto**

Senior Research Scientist, Dr. Kazuhide Kumakura
Senior Research Scientist, Dr. Kazuaki Furukawa

NTT Research Professor

Dr. Fujio Shimizu (The University of Electro-Communications) *
Prof. Shintaro Nomura (University of Tsukuba)
Prof. Kyo Inoue (Osaka University)

Materials Science Laboratory



Executive Manager,

Dr. Toshiki Makimoto
Dr. Keiichi Torimitsu*

Assistant Manager,

Dr. Satoru Suzuki

Thin-Film Materials Research Group:

Dr. Makoto Kasu (Group Leader)

Dr. Yasuyuki Kobayashi

Dr. Tetsuya Akasaka

Dr. Michal Kubovic*

Dr. Hideki Yamamoto

Dr. Yoshitaka Taniyasu

Dr. Kazuyuki Hiramata

Dr. Hisashi Sato

Dr. Chiun-Lung Tsai*

Low-Dimensional Nanomaterials Research Group:

Dr. Hiroki Hibino (Group Leader)

Dr. Fumihiko Maeda

Akio Tokura

Dr. Hiroo Omi

Dr. Shin-ichi Tanabe

Dr. Ken-ichi Kanzaki

Dr. Daisuke Takagi

Molecular and Bio Science Research Group:

Dr. Keiichi Torimitsu (Group Leader)

Dr. Keisuke Ebata

Dr. Akiyoshi Shimada

Toichiro Goto

Dr. Koji Sumitomo

Dr. Hiroshi Nakashima

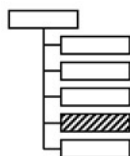
Dr. Youichi Shinozaki

Dr. Nahoko Kasai

Dr. Yoshiaki Kashimura

Dr. Aya Tanaka

Physical Science Laboratory



Executive Manager, **Dr. Hiroshi Yamaguchi**

Assistant Manager, Dr. Kenji Yamazaki
Takeshi Karasawa

Nanodevices Research Group:

Dr. Akira Fujiwara (Group Leader)

Dr. Yukinori Ono

Dr. Hiroyuki Kageshima

Dr. Katsuhiko Nishiguchi

Dr. Jin-ichiro Noborisaka

Dr. Mohammed A. H. Khalafalla*

Nanostructure Technology Research Group:

Dr. Hiroshi Yamaguchi (Group Leader)

Dr. Masao Nagase

Toru Yamaguchi

Dr. Hajime Okamoto

Dr. Koji Onomitsu

Dr. Imran Mahboob

Junzo Hayashi

Quantum Solid State Physics Research Group:

Dr. Koji Muraki (Group Leader)

Dr. Kiyoshi Kanisawa

Dr. Kyoichi Suzuki

Dr. Toshiaki Hayashi

Dr. Takeshi Ota

Dr. Norio Kumada

Dr. Keiko Takase

Dr. Ken-ichi Hitachi

Dr. Kei Takashina*

Dr. Gerardo Gamez

Dr. Kasper Grove-Rasmussen* Tadashi Saku

Superconducting Quantum Physics Research Group:

Dr. Kouichi Semba (Group Leader)

Dr. Hayato Nakano

Dr. Shiro Saito

Dr. Shin-ichi Karimoto

Hirofumi Tanaka

Dr. Kousuke Kakuyanagi

Dr. Alexandre Kemp

Dr. Xiaobo Zhu

Spintronics Research Group:

Dr. Tatsushi Akazaki (Group Leader)

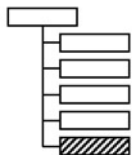
Dr. Yuichi Harada

Dr. Hiroyuki Tamura

Dr. Masumi Yamaguchi

Dr. Yoshiaki Sekine

Optical Science Laboratory



Executive Manager, **Dr. Yasuhiro Tokura**

Assistant Manager, Dr. Satoshi Sasaki

Quantum Optical State Control Research Group:

Dr. Yasuhiro Tokura (Group Leader)

Dr. Kaoru Shimizu

Dr. Makoto Yamashita

Dr. Hiroki Takesue

Dr. Kiyoshi Tamaki

Dr. Kensuke Inaba

Kazuhiro Igeta

Dr. Hiroyuki Shibata

Dr. Fumiaki Morikoshi

Daisuke Hashimoto

Masami Kumagai

Dr. Tetsuya Mukai

Dr. Toshimori Honjo

Dr. Ken-ichi Harada

Quantum Optical Physics Research Group:

Dr. Tetsufumi Sogawa (Group Leader)

Dr. Hidetoshi Nakano

Hidehiko Kamada

Dr. Katsuya Oguri

Dr. Guoqiang Zhang

Dr. Tadashi Nishikawa

Dr. Kouta Tateno

Dr. Atsushi Ishizawa

Dr. Keiko Kato

Dr. Hideki Gotoh

Dr. Takehiko Tawara

Dr. Haruki Sanada

Photonic Nano-Structure Research Group:

Dr. Masaya Notomi (Group Leader)

Dr. Atsushi Yokoo

Dr. Hideaki Taniyama

Dr. Kengo Nozaki

Dr. Eiichi Kuramochi

Dr. Takasumi Tanabe

Dr. Young-Geun Roh

Dr. Akihiko Shinya

Dr. Hisashi Sumikura

Distinguished Technical Members



Masaya Notomi was born in Kumamoto, Japan on February 16, 1964. He received his B.E., M.E. and Dr. Eng. degrees in applied physics from The University of Tokyo, Japan in 1986, 1988, and 1997, respectively. In 1988, he joined NTT Optoelectronics Laboratories. Since then, his research interest has been to control the optical properties of materials and devices by using artificial nanostructures, and engaged in research on semiconductor quantum wires/dots and photonic crystal structures. He has been in NTT Basic Research Laboratories since 1999, and is currently working on light-propagation control by use of various types of photonic crystals. From 1996-1997, he was with Linköping University in Sweden as a visiting researcher. He is also a guest associate professor of Tokyo Institute of Technology (2001-2009). He received IEEE/LEOS Distinguished Lecturer Award in 2006, JSPS (Japan Society for the Promotion of Science) prize in 2009, and Japan Academy Medal in 2009. He is a member of National University Corporation Evaluation Committee. He is also a member of the Japan Society of Applied Physics, IEEE, APS and OSA.



Akira Fujiwara was born in Tokyo, Japan on March 9, 1967. He received his B.S., M.S., and Ph.D. degrees in applied physics from The University of Tokyo, Japan in 1989, 1991, and 1994, respectively. In 1994, he joined NTT LSI Laboratories and moved to the Basic Research Laboratories in 1996. Since 1994, he has been engaged in research on silicon nanostructures and their application to single-electron devices. He was a guest researcher at the National Institute of Standards and Technology (NIST), Gaithersburg, MD, USA during 2003-2004. He received the SSDM Young Researcher Award in 1998, SSDM Paper Award in 1999, and Japanese Journal of Applied Physics (JJAP) Paper Awards in 2003 and 2006. He was awarded the Young Scientist Award from the Minister of MEXT (Ministry of Education, Culture, Sports, Science, and Technology) in 2006. He is a member of the Japan Society of Applied Physics and the IEEE.



Koji Muraki was born in Tokyo, Japan in 1965. He received his B.S., M.S., and Ph.D. degrees in applied physics from The University of Tokyo, Japan, in 1989, 1991, and 1994, respectively. In 1994, he joined Basic Research Laboratories, Nippon Telegraph and Telephone Corporation, Kanagawa, Japan. Since then, he has been engaged in the growth of high-mobility heterostructures and the study of highly correlated electronic states realized in such structures. He was a guest researcher at Max-Planck Institute, Stuttgart, Germany during 2001-2002. He is a member of the Physical Society of Japan and Japan Society of Applied Physics.

Advisory Board (2009 Fiscal Year)

Name	Affiliation
Prof. Gerhard Abstreiter	Walter Schottky Institute, Germany
Prof. Boris L. Altshuler	Department of Physics, Columbia University, U.S.A.
Prof. Serge Haroche	Département de Physique, De l'Ecole Normale Supérieure, France
Prof. Mats Jonson	Department of Physics, Göteborg University, Sweden
Prof. Anthony J. Leggett	Department of Physics, University of Illinois at Urbana-Champaign, U.S.A.
Prof. Johan E. Mooij	Kavli Institute of Nanoscience, Delft University of Technology, the Netherlands
Prof. John F. Ryan	Clarendon Laboratory, University of Oxford, U.K.
Prof. Klaus von Klitzing	Max-Planck-Institut für Festkörperforschung, Germany
Prof. Theodor W. Hänsch	Max-Planck-Institut für Festkörperforschung, Germany

Invited / Guest Scientists (2009 Fiscal Year)

Name	Affiliation	Period
Prof. Alexander Tzalenchuk	National Physical Laboratory, U.K.	Apr. 2009 – May 2009
Dr. Stefan Folsch	Paul-Drud-Institute, Germany	Oct. 2009 – Nov. 2009
Prof. Christos Flytzanis	Laboratoire Pierre Aigrain Ecole Normale Supérieure, France	Sep. 2009 – Dec. 2009
Assoc. Prof. Takaaki Koga	Hokkaido University, Japan	Jan. 2007 – Dec. 2009
Dr. Hideomi Hashiba	Institute of Quantum Science, Nihon University, Japan	Jul. 2008 – Mar. 2010
Dr. Lars Tiemann	Japan Science and Technology Agency (JST), Japan	Apr. 2009 – Mar. 2010
Dr. Shoko Utsunomiya	National Institute of Informatics, Japan	May 2009 – Mar. 2010
Dr. Yoichi Chizaki	Advanced Industrial Science And Technology (AIST)	Feb. 2010 – Mar. 2010

Overseas Trainees (2009 Fiscal Year)

Name	Affiliation	Period
Christoph Hufnagel	University of Heidelberg, Germany	Jun. 2006 – Jun. 2009
Stefano Salvatore	Technical University, Milan, Italy	Jan. 2009 – Aug. 2009
Maarten Nijland	University of Twente, the Netherlands	Jan. 2009 – Apr. 2009
Corentin Durand	University of Lille/ ISEN, France	Feb. 2009 – Jul. 2009
Pauline Renoux	INSA (Institut National des Sciences Appliquées de Toulouse), France	Feb. 2009 – Aug. 2009
Laurent-Daniel Haret	Institut d'Optique Graduate School, France	Mar. 2009 – Aug. 2009
Jelena Baranovic	University of Oxford, U.K.	May 2009 – Jun. 2009
Chia-Yuan Chang	National Chiao-Tung University, Taiwan	May 2009 – Feb. 2010
Chien-Yao Lu	University of Illinois at Urbana-Champaign, U.S.A.	May 2009 – Aug. 2009
Paul-Christiaan Spruijtenburg	University of Twente, Enschede, the Netherlands	May 2009 – Oct. 2009
Man-Hong Yung	University of Illinois at Urbana-Champaign, U.S.A.	Jun. 2009 – Jul. 2009
Paul Nation	Dartmouth College, Hanover, New Hampshire U.S.A.	Jun. 2009 – Aug. 2009
Timothee Martiel	ESPCI (Ecole Supérieure de Physique et de Chimie Industrielle), France	Jul. 2009 – Dec. 2009
Emmanuel Flurin	ESPCI (Ecole Supérieure de Physique et de Chimie Industrielle), France	Jul. 2009 – Dec. 2009
Myrtille Hunault	ESPCI (Ecole Supérieure de Physique et de Chimie Industrielle), France	Jul. 2009 – Dec. 2009
Stefano Pugnetti	Scuola Normale Superiore-Pisa, Italy	Aug. 2009 – Sep. 2009
Oliver Pirquet	University of Victoria, Canada	Sep. 2009 –
Arianna McAllister	University of Ottawa, Canada	Sep. 2009 –
Jessica Sparks	University of Waterloo, Canada	Sep. 2009 –
Fabio Massimo Zennaro	Politecnico di Milano, Italy	Jan. 2010 –
Gary Wolfowicz	ENS (Ecole Normale Supérieure de Cachan), France	Jan. 2010 –
David Framil Carpeno	Complutense Univeristy of Madrid, Spain	Jan. 2010 –

Name	Affiliation	Period
Jan Fiala	Czech Technical University in Prague, Czech Republic	Jan. 2010
Juan Manuel Agudo Carrizo	UPV(Polytechnic University of Valencia), Spain	Jan. 2010
Romain Duval	INSA (Institut National des Sciences Appliquées deToulouse), France	Feb. 2010
Raymond Davis	Royal Holloway, University of London, U.K.	Feb. 2010 – Mar. 2010
Aimée Broughton	University of Oxford, U.K.	Feb. 2010 – Mar. 2010
Laura Spencer	University of Oxford, U.K.	Feb. 2010 – Mar. 2010
Kylie Ellis	The University of Adelaide, Australia	Mar. 2010
Yuichiro Matsuzaki	University of Oxford, U.K.	Mar. 2010

Domestic Trainees (2009 Fiscal Year)

Name	Affiliation	Period
Hiroshi Sakai	Tokyo University of Science, Japan	Apr. 2009 – Mar. 2010
Kenji Yamaya	Tokyo University of Science, Japan	Apr. 2009 – Mar. 2010
Hiroyuki Wakahara	Keio University, Japan	Apr. 2009 – Mar. 2010
Akira Wada	Tohoku University, Japan	Apr. 2009 – Mar. 2010
Kohei Morita	Kyushu University, Japan	Apr. 2009 – Mar. 2010
Satoru Miyamoto	Keio University, Japan	Apr. 2009 – Mar. 2010
Kuniaki Yamada	Keio University, Japan	Apr. 2009 – Mar. 2010
Norihito Kitajima	The University of Tokyo, Japan	Apr. 2009 – Mar. 2010
Yasuhiko Oda	The University of Tokyo, Japan	Apr. 2009 – Mar. 2010
Takayuki Watanabe	Tohoku University, Japan	Apr. 2009 – Mar. 2010
Takashi Kobayashi	Tohoku University, Japan	Apr. 2009 – Mar. 2010
Yuma Okazaki	Tohoku University, Japan	Apr. 2009 – Mar. 2010
Kenichiro Kusudo	The University of Tokyo, Japan	Apr. 2009 – Mar. 2010
Naoyuki Masumoto	The University of Tokyo, Japan	Apr. 2009 – Mar. 2010
Hiroshi Kamata	Tokyo Institute of Technology, Japan	Apr. 2009 – Mar. 2010
Tomohiro Nagase	Tokyo Institute of Technology, Japan	Apr. 2009 – Mar. 2010
Shun Takahashi	The University of Tokyo, Japan	Apr. 2009 – Mar. 2010
Haruki Kiyama	The University of Tokyo, Japan	Apr. 2009 – Mar. 2010
Atsufumi Inoue	The University of Tokyo, Japan	Apr. 2009 – Mar. 2010
Yasushi Kanai	The University of Tokyo, Japan	Apr. 2009 – Mar. 2010
Tatsuki Takakura	The University of Tokyo, Japan	Apr. 2009 – Mar. 2010
Shintaro Takada	The University of Tokyo, Japan	Apr. 2009 – Mar. 2010
Takafumi Fujita	The University of Tokyo, Japan	Apr. 2009 – Mar. 2010
Yusuke Kondo	The University of Tokyo, Japan	Apr. 2009 – Mar. 2010
Jun Yoneda	The University of Tokyo, Japan	Apr. 2009 – Mar. 2010
Ryota Koibuchi	Tokyo University of Science, Japan	Apr. 2009 – Mar. 2010
Hiroki Morishita	Keio University, Japan	Apr. 2009 – Mar. 2010
Yu Morikawa	University of Tsukuba, Japan	Apr. 2009 – Mar. 2010
Hiroshi Takahashi	Tokyo Institute of Technology, Japan	Apr. 2009 – Mar. 2010

Name	Affiliation	Period
Tetsuya Miyawaki	Tohoku University, Japan	Apr. 2009 – Mar. 2010
Akira Oiwa	The University of Tokyo, Japan	Apr. 2009 – Mar. 2010
Michihisa Yamamoto	The University of Tokyo, Japan	Apr. 2009 – Mar. 2010
Monica Crasiun	The University of Tokyo, Japan	Apr. 2009 – Oct. 2009
Saverio Russo	The University of Tokyo, Japan	Apr. 2009 – Oct. 2009
Russell Deacon	The University of Tokyo, Japan	Apr. 2009 – Mar. 2010
Allison Giles Daniel	The University of Tokyo, Japan	Apr. 2009 – Mar. 2010
Bäuerle Christopher	The University of Tokyo, Japan	Apr. 2009 – Jun. 2009
Tadakiyo Seki	Osaka University, Japan	May 2009 – Feb. 2010
Taiga Harada	Keio University, Japan	Aug. 2009
Keitaro Yamagami	Nagaoka University of Technology, Japan	Oct. 2009 – Feb. 2010
Motoki Tateishi	Nagaoka University of Technology, Japan	Oct. 2009 – Feb. 2010
Hiroki Shioya	The University of Tokyo, Japan	Jan. 2010 – Mar. 2010

I . Research Topics

Overview of Research in Laboratories

Materials Science Laboratory

Toshiki Makimoto

The Materials Science Laboratory (MSL) aims at producing new functional materials and designing of advanced device based on novel materials and biological function. Controlling the configuration and coupling of atoms and molecules is our approach to accomplish these goals.

We have three research groups covering from thin film materials, such as nitride semiconductors, diamond, graphene, and superconductors, to biological molecules, such as receptor proteins and lipid bilayers. The characteristic feature of MSL is the effective sharing of the unique nanofabrication and measurement techniques of each group. This enables fusion of research fields and techniques, which leads to innovative material research for the future information technology.

We promote collaborations with domestic and international organizations, such as the collaboration with Oxford University for bio-nano research, to develop a firm basis of basic science.

Physical Science Laboratory

Hiroshi Yamaguchi

We are studying semiconductor and superconductor-based solid-state devices, which will have a revolutionary impact on communication and information technologies in the 21st century. In particular, we promote research of nanoscale devices fabricated using high-quality crystal growth and fine lithographic techniques.

The five groups in our laboratory are working in the following areas: precise and dynamical control of single electrons, nanodevices operating with ultra low power consumption, novel nanomechanical systems utilizing mechanical degrees of freedom in solid-state architectures, coherent quantum control of semiconductor and superconductor systems, carrier interactions in semiconductor hetero- and nanostructures, atom chips, spintronics manipulating both electron and nuclear spins. We also promote the studies of cutting-edge nanolithography techniques, high-quality crystal growth, and theoretical studies including first-principle calculations.

Optical Science Laboratory

Yasuhiro Tokura

This laboratory aims for the development of core-technologies that will innovate on optical communications and optical signal processing, and seeks fundamental scientific progresses. The groups in our laboratory are working for the quantum state control by very weak light, the search for intriguing phenomena using very intensive and short pulse light, and very small optical integrated circuits using two-dimensional photonic crystals, based on the optical properties of semiconductor nanostructures like a quantum dot.

In this year, we realized quantum interference in two entangled photon pairs from silicon wire waveguides, lateral growth of semiconductor (InGaAs) nanowires, and an optical switch functions at the power of sub-femto Joule by a photonic crystal nano-cavity.

Improvement of H-terminated Diamond FETs in NO₂ Atmosphere

Michal Kubovic and Makoto Kasu
Materials Science Laboratory

Diamond transistors are expected to provide the best performance among semiconductors in high-frequency high-power operation because diamond has very high carrier velocity, the highest breakdown electric field strength, and the highest thermal conductivity. We reported the highest cut-off frequencies of f_T of 45 GHz, f_{max} of 120 GHz, and the highest RF output power density of 2.1 W/mm at 1 GHz [1]. However, the p-type doping mechanism of the hydrogen termination used in diamond transistors has not been clarified and the hole concentration has been limited at $1 \times 10^{13} \text{ cm}^{-2}$.

We have experimentally clarified that nitrogen dioxide (NO₂) is the most beneficial p-type dopant for H-terminated diamond [2-4]. As shown in Fig. 1, when NO₂ gas is adsorbed onto H-terminated diamond, the hole concentration increased greatly. With 300 ppm NO₂, the maximum hole concentration reached $2.3 \times 10^{14} \text{ cm}^{-2}$, a value that is 20 times higher than the reported value in air. With this technology, we fabricated H-terminated diamond FETs whose drain current is 1.8 times higher due to a decrease in source resistance [Fig. 2(a)] and whose power-gain cut-off frequency (f_{maxU}) is 1.5 times higher [Fig. 2(b)] than those in air [2].

This work was partly supported by the SCOPE project of the Ministry of Internal Affairs and Communications, Japan.

- [1] M. Kasu, K. Ueda, Y. Yamauchi et al., *Diamond Relat. Mater.* **16** (2007) 1010.
- [2] M. Kubovic and M. Kasu, *Appl. Phys. Express* **2** (2009) 086502.
- [3] M. Kubovic, M. Kasu, and H. Kageshima, *Appl. Phys. Lett.* **96** (2010) 052101.
- [4] M. Kubovic, M. Kasu, H. Kageshima, and F. Maeda, *Diamond Relat. Mater.* (in press).

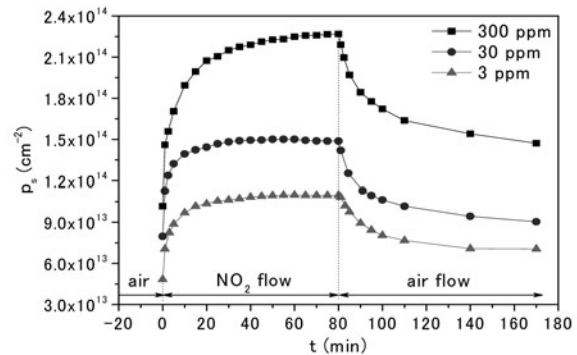


Fig. 1. Time evolution of hole sheet concentration during NO₂ adsorption and desorption.

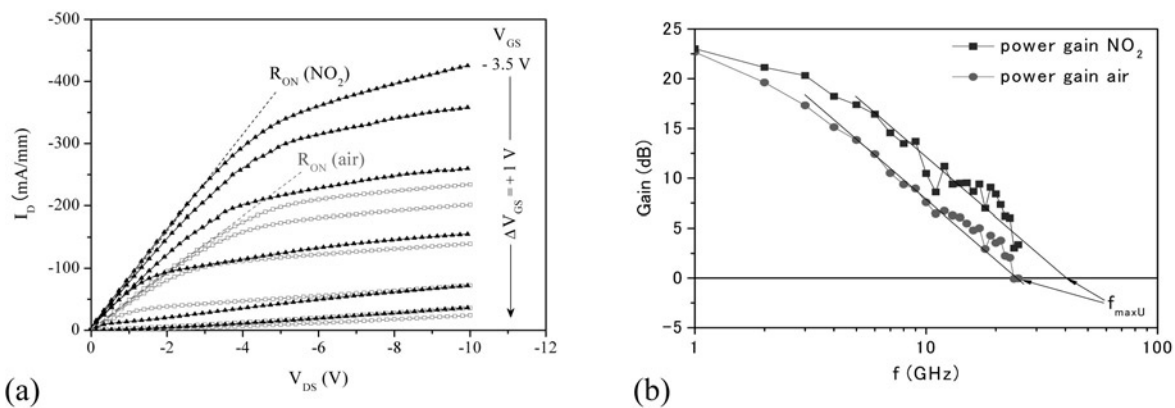


Fig. 2. (a) Drain current-voltage characteristics and (b) frequency dependence of power gain (unilateral gain) before and after NO₂ adsorption.

Single-crystal AlN (0001)/diamond (111) Heterostructure

Kazuyuki HIRAMA, Yoshitaka TANIYASU, and Makoto KASU
Materials Science Laboratory

Both aluminum nitride (AlN) and diamond have wide bandgaps: 6.0 eV for AlN and 5.5 eV for diamond. On the other hand, they have opposite doping characteristics. For AlN, n-type doping is easier than p-type doping, while for diamond, p-type doping is easier than n-type doping. The AlN/diamond heterostructure is expected to combine the features of both materials and appears promising for achieving high-efficiency deep-ultraviolet light-emitting diodes and high-power electron devices. The key to realizing these devices is single-crystal growth of AlN on diamond. However, to date, due to the difference in the crystal structures (hexagonal structure for AlN; cubic structure for diamond), AlN layers grown on diamond substrates have had multi-domain structures [1].

Here, using diamond (111) plane, we grew the AlN layer on the diamond substrate because the atomic bonding configuration of the hexagonal AlN (0001) plane is similar to that of the cubic diamond (111) plane. Figure 1 shows the X-ray pole figures of AlN (0002) and (10 $\bar{1}1$) planes. In Figure 1(a), a strong diffraction peak was only observed at $\Psi = 0^\circ$. This indicates that the AlN [0001] direction was oriented normal to the diamond (111) surface. In Figure 1(b), at $\Psi = 62^\circ$, we only observed six diffraction peaks, which are attributed to six equivalent (10 $\bar{1}1$) planes for hexagonal AlN. These results indicate single-crystal growth of the AlN (0001) layer on the diamond (111) substrate.

In the cross-section TEM image at the heterointerface (Fig. 2), an abrupt AlN/diamond interface was observed without any interface layer. This confirms that the single-crystal AlN (0001) layer epitaxially grows from the nucleation step just on the diamond (111) surface. At the AlN(0001)/diamond(111) interface, there are two possible bonds, C-N or C-Al bonds. Because the bond energy of the C-N bond (3.1 eV/bond) is stronger than that of the C-Al bond (2.6 eV/bond), the C-N bond is preferentially formed at the AlN/diamond interface. As a result, the AlN layer grown on diamond has Al polarity.

For the AlN(0001)/diamond(111) heterostructure, the in-plane epitaxial relationship is $[10\bar{1}0]_{\text{AlN}} \parallel [1\bar{1}0]_{\text{diamond}}$, although the lattice mismatch for $[10\bar{1}0]_{\text{AlN}} \parallel [1\bar{1}0]_{\text{diamond}}$ is larger than that for $[11\bar{2}0]_{\text{AlN}} \parallel [1\bar{1}0]_{\text{diamond}}$. The in-plane epitaxial relationship can be explained in terms of interface energy. The bond densities at the interface for $[10\bar{1}0]_{\text{AlN}} \parallel [1\bar{1}0]_{\text{diamond}}$ and $[11\bar{2}0]_{\text{AlN}} \parallel [1\bar{1}0]_{\text{diamond}}$ are $2.7 \times 10^{14} \text{ cm}^{-2}$ and $2.2 \times 10^{14} \text{ cm}^{-2}$, respectively. Because $[10\bar{1}0]_{\text{AlN}} \parallel [1\bar{1}0]_{\text{diamond}}$ has a higher bond density and therefore lower interfacial energy, $[10\bar{1}0]_{\text{AlN}} \parallel [1\bar{1}0]_{\text{diamond}}$ is energetically preferred for the single-crystal AlN (0001) layer on diamond (111) surface.

[1] K. HIRAMA, Y. TANIYASU, and M. KASU, *Jpn. J. Appl. Phys.* **49** (2010) 04DH01.

[2] Y. TANIYASU and M. KASU, *J. Cryst. Growth* **311** (2009) 2825.

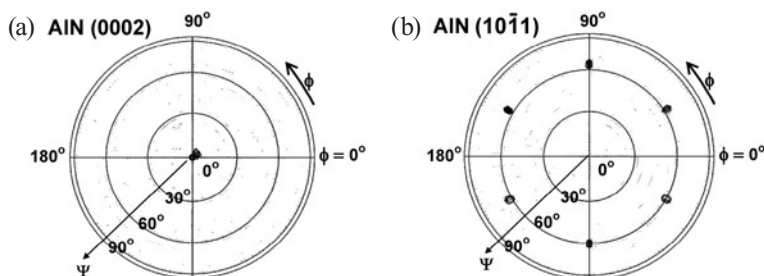


Fig. 1. XRD pole figures of (a) AlN (0002) and (b) AlN (10 $\bar{1}1$) planes of the AlN grown on diamond (111).

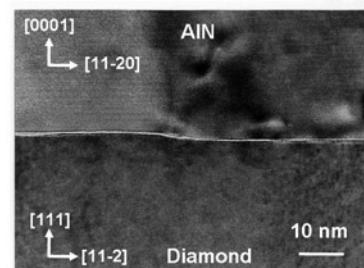


Fig. 2. TEM image at the AlN (0001)/diamond(111) heterointerface.

Step-free GaN films Grown by Selective-area Metalorganic Vapor Phase Epitaxy

Tetsuya Akasaka, Yasuyuki Kobayashi, and Makoto Kasu
Materials Science Laboratory

Step-free surfaces of GaN-related nitride semiconductors have been strongly desired for studying growth mechanisms and for achieving the abrupt hetero-interfaces necessary for nitride-based devices, such as laser diodes, resonant tunneling diodes, and cascade lasers. Previously reported surfaces of nitride semiconductors, however, showed a high density of monolayer steps originating from crystal defects (dislocations). Here, we report the first successful fabrication of step-free GaN surfaces, which are covered with single wide atomic terraces without any monolayer steps. The step-free surfaces were obtained by using GaN substrates with low dislocation densities and by optimizing growth conditions, such as temperature, growth rates, and the V/III ratio [1].

First, a SiO₂ mask was deposited on a GaN (0001) substrate with low dislocation density ($\sim 10^6$ cm⁻²). Then, the SiO₂ mask was patterned by photolithography so as to have many hexagonal openings with the diameter of 16 μ m. Finally, selective-area metalorganic vapor phase epitaxy (SA-MOVPE) of GaN films was performed onto the mask-patterned GaN substrate. Source gases were ammonia and trimethylgallium (TMG).

Figure 1 shows an atomic force microscopy (AFM) image of a GaN surface fabricated at 940°C and at the TMG flow rate of 2.6×10^{-5} mol/min. The surface has a single wide terrace over almost its whole area (step-free surface) except at the edges and there are no screw-type dislocations within the GaN hexagon. On the other hand, a GaN surface fabricated by conventional MOVPE exhibited a high density of monolayer steps with an average interstep distance of ~ 0.1 μ m (Fig. 2). In addition, a GaN surface fabricated by SA-MOVPE under non-optimized growth conditions had several ten monolayer steps.

In conclusion, we fabricated step-free GaN surfaces with the diameter of 16 μ m by SA-MOVPE using GaN substrates with low dislocation density under optimized conditions.

[1] T. Akasaka, Y. Kobayashi, and M. Kasu, *Appl. Phys. Express* **2** (2009) 091002.

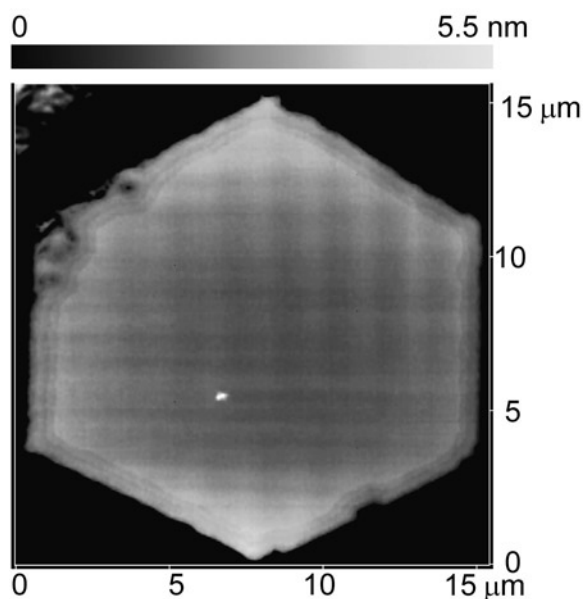


Fig. 1. AFM image of step-free GaN surface with diameter of 16 μ m grown by selective-area metalorganic vapor phase epitaxy.

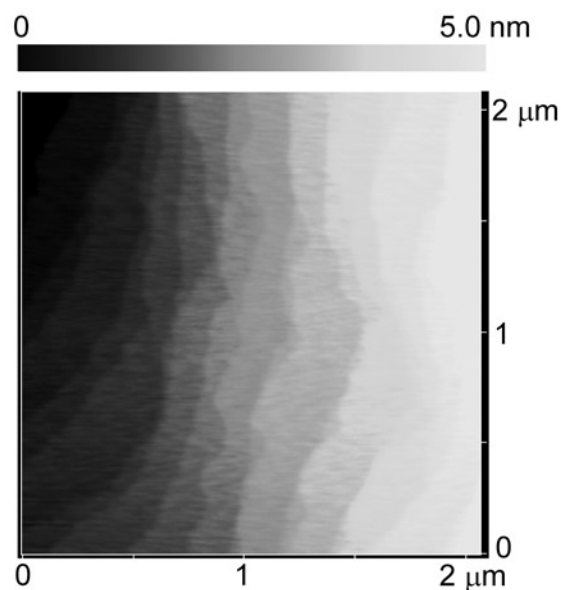


Fig. 2. AFM image of GaN surface grown by conventional metalorganic vapor phase epitaxy.

Synthesis of the Parent Compound Superconductors RE_2CuO_4 by MBE and Specially-designed Post-reduction

Hideki Yamamoto, Osamu Matsumoto*, Keitaro Yamagami, and Michio Naito*
Materials Science Laboratory, *Tokyo Univ. of Agricul. & Technol.

It is commonly believed that the parent compounds of high- T_c cuprates are, universally, Mott insulators (charge-transfer insulators). There has been, however, accumulating evidence that indicates a series of parent compounds $T'-RE_2CuO_4$ [RE stands for rare earth element] are superconductors with T_c even exceeding 30 K when they are optimally synthesized [1]. Most of the recent progress has been achieved by using the metal-organic decomposition (MOD) method [1]. Most likely, this originates from the necessity of removing impurity interstitial oxygen while simultaneously preserving regular oxygen sites occupied, which is a prerequisite for achieving superconductivity in square-coplanar CuO_2 plane. It appears that this requirement is easier to be fulfilled in the MOD films due to rather small grains in them [2], which in turn makes it difficult to reproduce the results using other synthesis methods. In this study, we systematically investigated the post-reduction process using MBE-grown $T'-RE_2CuO_4$ ($RE=Pr, Nd$) films on $SrTiO_3$ (001) substrates for an easier reproduction through a better understanding of the process.

Figure 1 shows several important parameters in the growth and post-reduction procedures. To make the parent compounds superconducting, a specially-designed 2-step reduction process was necessary, as in the case of MOD films. By optimizing oxygen partial pressure and annealing temperature with constant duration, the MBE-grown RE_2CuO_4 ($RE=Pr, Nd$) films show superconductivity (Fig. 2) [3].

These findings are useful for synthesizing bulk specimens of the parent compound superconductors, which makes evaluation of oxygen stoichiometry feasible. They are also useful for synthesizing the thin-film specimens through an all-UHV process, with which a direct observation of electronic structure by photoemission spectroscopy becomes possible. Both will lead us toward the true electronic phase diagram for high- T_c cuprates.

- [1] O. Matsumoto et al., Phys. Rev. B **79** (2009) 100508; Physica C **469** (2009) 924.
[2] O. Matsumoto, A. Tsukada, H. Yamamoto, T. Manabe, and M. Naito, Physica C (in press).
[3] H. Yamamoto, A. Tsukada, O. Matsumoto, and M. Naito, Physica C (in press).

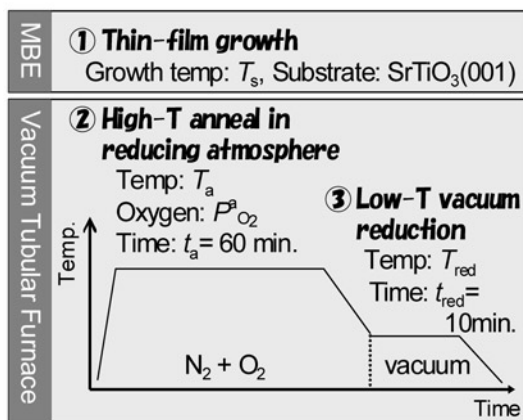


Fig. 1. Parameters in MBE growth and post-reduction of RE_2CuO_4 thin films.

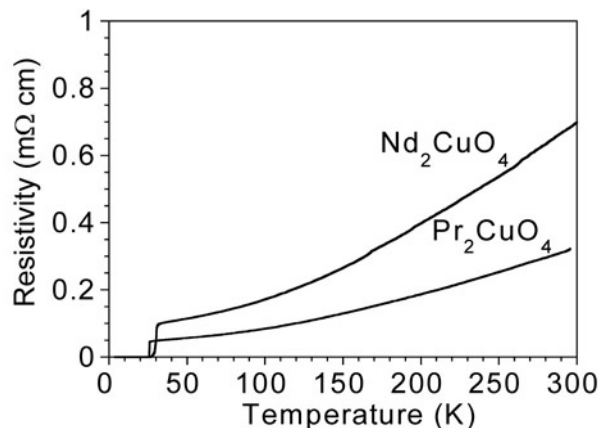


Fig. 2. ρ - T characteristics of MBE-grown Nd_2CuO_4 and Pr_2CuO_4 thin films.

Growth of Graphene by Gas-source Molecular Beam Epitaxy

Fumihiko Maeda and Hiroki Hibino
Materials Science Laboratory

Because of the excellent electrical performance of graphene, such as a highest carrier mobility at room temperature, it is recognized as one of the most promising candidates for the next-generation of electronics materials. However, for its practical application, a remaining challenge is the formation of graphene films with high quality and wafer-scale size to achieve compatibility with a large-scale manufacturing process. To meet this challenge, we propose a new approach for forming wafer-scale graphene, which is based on gas-source molecular beam epitaxy (MBE). In this method, the substrate is not restricted to specific ones as it is in other promising methods, such as graphene formation by means of epitaxy on SiC [1] or on transition metals [2]. We report here a demonstration of the gas-source MBE to show the feasibility of our new approach for the formation of graphene [3].

In this experiment, about three atomic layers of graphene, prepared by high-temperature annealing of 6H-SiC(0001) under an ultra-high vacuum, were used as a substrate for the homoepitaxial growth. This substrate was heated to 620°C and cracked ethanol was supplied as a growth material. After this growth, *in situ* x-ray photoelectron spectroscopy (XPS) measurements indicated that about four monolayers of graphitic material were grown. The cross-sectional transmission electron microscope image in Fig. 1 shows that this grown graphitic material has a layered structure. These results show that graphene was grown. Meanwhile, in the Raman spectra of the samples with and without the growth [Fig. 2], we observed changes in the peak shape of the 2D-band and an increase in the intensity of the G-band. This result supports the increase of graphene thickness by the growth. However, a remarkable D-band peak was also observed after the growth, indicating that the domain size of the graphene is small. These results indicate that our new approach is feasible for the formation of wafer-scale graphene and that it would be compatible with device fabrication processes, although improvement in the crystal quality is needed.

[1] A. J. van Bommel, J. E. Crombeen, and A. van Tooren, *Surf. Science* **48** (1975) 463.

[2] L. C. Isett and J. M. Blakely, *Surf. Science* **58** (1976) 397.

[3] F. Maeda and H. Hibino, *Phys. Status Solidi B* **247** (2010) 916.

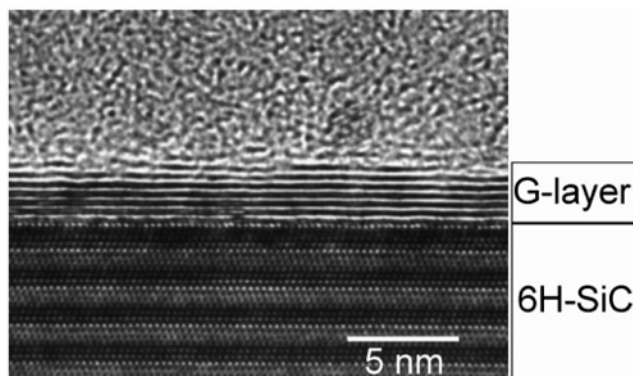


Fig. 1. Cross-sectional transmission electron microscope image after MBE growth.

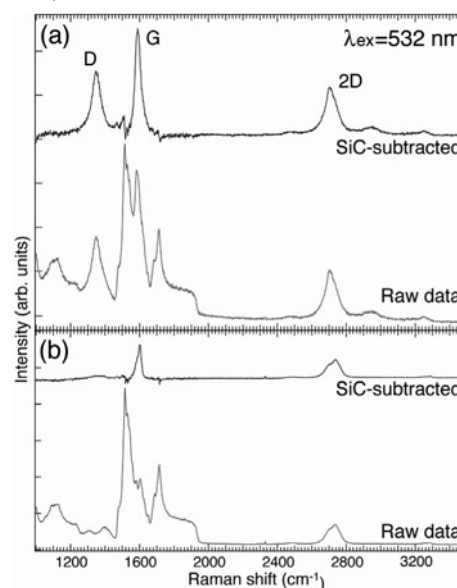


Fig. 2. Raman spectra of the samples (a) with and (b) without the overlayer growth.

Stability-instability Transition of Reaction Fronts in Thermal Silicon Oxidation

Hiroo Omi and Hiroyuki Kageshima*

Materials Science Laboratory, *Physical Science Laboratory

The SiO₂/Si(001) has been one of the most important interfaces in silicon semiconductors and related silicon nanotechnologies. Due to its significance, therefore, much works have been done to understand the roughening mechanism of silicon oxidation not only on surface [1], but also at interface [2]. In this work, morphological evolution at the interface between the Si(001) substrate and the thermal SiO₂ film grown at the oxidation temperature between 1000 and 1380°C in a dilute oxygen/Ar atmosphere were systematically studied by atomic force microscopy (AFM) and synchrotron radiation X-ray reflectivity (XRR) measurements as a function of oxidation temperature and time, and miscut angle of the substrates. The AFM results show that thermal oxidation causes interface roughening with forming step-terrace structures (Region II in Fig. 1) between 1150-1250°C and then smoothed during the thermal oxidation above 1250°C (Region III in Fig. 1) independent of miscut angles below 4 deg. The interface roughening and smoothing possibly relates to the temperatures of which determine the viscosity of the growing SiO₂ film. The XRR measurements on the as-grown silicon oxide films support the presence of the temperature dependences. As seen in Fig. 2, σ_{i-s} is constant in region (I), but it becomes extremely rough from $T_{ox} = 1150^\circ\text{C}$ with the roughness (RMS) reaching a maximum at $T_{ox} = 1250^\circ\text{C}$ in region (II). It then gradually becomes smaller in region (III), in accordance with the AFM results in Fig. 1. The temperature dependence of interface and surface roughening in Fig. 2 indicates that there is an apparent temperature dependent mechanism of how the strain induced by oxidation relieves at the growing interface between Si and silicon oxide film and in the whole region of silicon oxide films.

- [1] *Fundamental Aspects of Silicon Oxidation*, edited by Y. J. Chabal (Springer, 2001).
 [2] H. Omi, H. Kageshima, and M. Uematsu, Phys. Rev. Lett. **97** (2006) 01602.
 [3] H. Omi, H. Kageshima, T. Kawamura, M. Uematsu, Y. Kobayashi, S. Fujikawa, Y. Tsusaka, Y. Kageshima, and J. Matsui, Phys. Rev. B. **79** (2009) 245319.

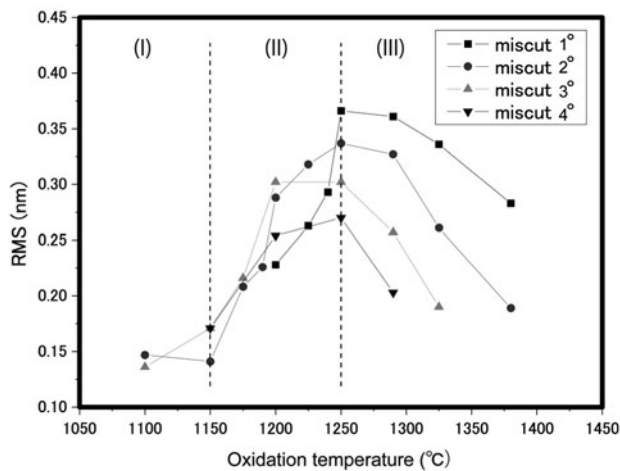


Fig. 1. RMS vs oxidation temperature.

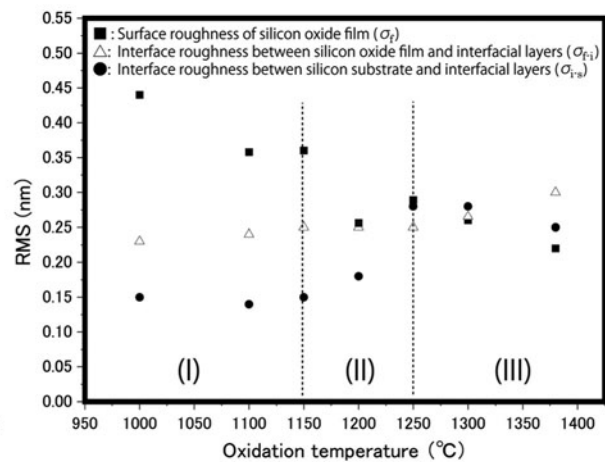


Fig. 2. Surface and interface roughness, obtained by XRR.

Stacking Domains in Epitaxial Bilayer Graphene

Hiroki Hibino¹, Seigi Mizuno², and Hiroyuki Kageshima³

¹Materials Science Laboratory, ²Kyushu University, and ³Physical Science Laboratory

Few-layer graphene (FLG) is attracting intense attention as a future electronics material due to its superior electronic transport properties. Epitaxial FLG grown on SiC substrates by thermal decomposition can be easily scaled up and is promising for device integration. We have so far established a method of determining the number of graphene layers microscopically using low-energy electron microscopy (LEEM) [1] and have succeeded in growing bilayer graphene a few micrometers in size. In this work, we clarified the domain structures in bilayer graphene [2].

Figure 1 shows LEEM images of FLG 1-3 layers thick grown on 4H-SiC(0001). Bilayer graphene looks continuous in the bright-field LEEM image [Fig. 1(a)] obtained using the specularly reflected (0,0) beam. However, the dark-field LEEM images [Figs. 1(b) and 1(c)] obtained using the diffracted (1,0) and (0,1) beams clearly show that bilayer graphene contains two types of domains. The contrast of the two domains are reversed between the (1,0) and (0,1) dark-field LEEM images, indicating that these domains have three-fold symmetry. Monolayer graphene has six-fold symmetry, and two carbon atoms are located at A and B sites in a unit cell. On the other hand, as shown in Fig. 2, bilayer graphene can have two types of stacking orders with three-fold symmetry: AB stacking in which a B' carbon atom is on an A carbon atom and BA (usually called AC) stacking in which an A' carbon atom is on a B carbon atom. Therefore, we speculate that the two types of domains seen experimentally correspond to the AB and AC stackings. To confirm this, we measured the energy dependence of the intensities of the dark-field LEEM images for the two domains and compared it to the calculated energy dependence of the (1,0) and (0,1) low-energy electron diffraction intensities for bulk graphite. Good agreement between these two energy dependences proves that there are stacking domains in bilayer graphene. The stacking domain structures can affect the electronic transport properties in FLG. The formation mechanism and condition for growing a single stacking domain are the next targets.

This work was supported by KAKENHI.

[1] H. Hibino et al., Phys. Rev. B **77** (2008) 075413.

[2] H. Hibino et al., Phys. Rev. B **80** (2009) 085406.

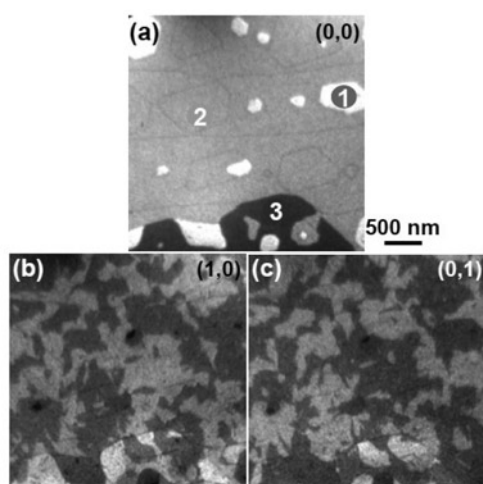


Fig. 1. (a) Bright-field and (b)-(c) dark-field LEEM images of epitaxial FLG. In (a), 1-3 indicate the number of graphene layers. Electron beam energies were (a) about 5 eV and (b)-(c) about 58 eV.

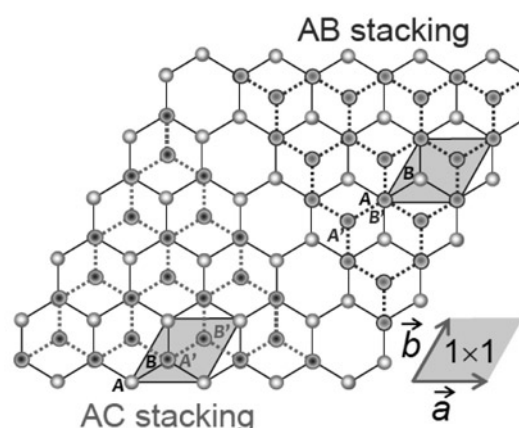


Fig. 2. Schematic illustration of AB and AC stackings in bilayer graphene.

Carbon Nanotube Synthesis from Diamond

Daisuke Takagi and Yoshihiro Kobayashi*
Materials Science Laboratory, *Osaka University

We have succeeded in growing carbon nanotubes (CNTs) from diamond. CNTs are promising as future base components in many industrial fields due to their various superior properties, such as low weight, high mechanical strength, and good electrical/thermal conductivities. So far, Fe, rare metals like Co and Ni, and noble metals like Au, Ag, and Pt have been used as effective catalysts for CNT synthesis. However, because these metal catalyst particles easily lose their catalytic activities due to aggregation/fusion and reaction with substrates, they are not suitable for high-density CNT growth. Furthermore, because these metal catalyst particles are in a liquid phase at the single-wall CNT (SWCNT) growth temperatures, they cannot be used to precisely control the CNT structure, especially the chirality. Diamond is free from aggregation/fusion and is in a solid phase at the growth temperatures. Therefore, we hope diamond will make it possible to grow CNTs with a precisely controlled structure.

In this work, we clarified that the CNT synthesis from diamond by chemical vapor deposition (CVD) requires (1) the use of nanodiamond particles with a diameter smaller than 5 nm [1]; (2) removal of the graphite formed on the nanoparticle surface; and (3) the use of gases that thermally decomposed easily, such as ethanol vapor and acetylene, as the carbon feed stock [2]. Transmission electron microscopy (TEM) images [Figs. 1(a) and 1(b)] and the Fourier transform pattern [Fig. 1(c)] obtained from Fig. 1(b) indicate that SWCNTs are grown from nanodiamond particles. Scanning electron microscopy (SEM) image in Fig. 1(d) indicates that SWCNTs can be grown from three-dimensionally accumulated nanodiamond particles. This means that the nanodiamond particles were in the solid phase at the CVD ambient conditions and did not aggregate. It is known that, in metal-catalyzed CNT growth, carbon atoms are supplied to the CNT through bulk diffusion of carbon atoms in the particle. On the other hand, CNT growth from nanodiamond particles must be promoted by surface diffusion of carbon atoms.

Nanodiamond particles are produced at low cost and have catalyst activities as high as metal nanoparticles. The nanodiamond particles offer the possibility of not only low-cost, high-density growth of SWCNT but also precise control of the structure of SWCNT.

[1] E. Ōsawa, *Diamond Relat. Mater.* **16** (2007) 2018.

[2] D. Takagi et al., *J. Am. Chem. Soc.* **131** (2009) 6922.

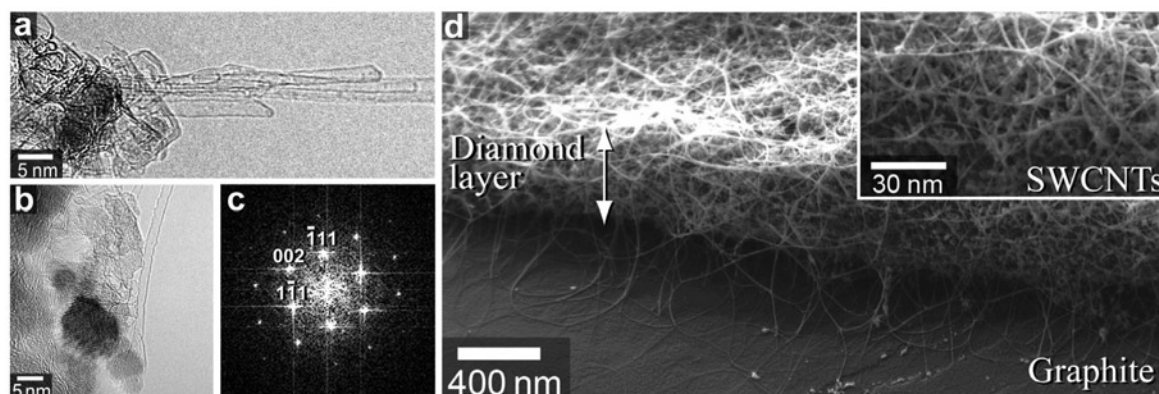


Fig. 1. (a) TEM image of SWCNTs and (b) TEM image of a SWCNT and nanodiamond particle. (c) Fourier transform pattern obtained from (b). (d) SEM image of SWCNTs grown from three-dimensionally accumulated nanodiamond particles on graphite substrate.

Effect of Mg^{2+} on Neural Activity

Keiichi Torimitsu
Materials Science Laboratory

It is well known that magnesium ion (Mg^{2+}) plays an important role in biological functions, similar to that of calcium ion (Ca^{2+}). It would be useful to understand the effect of Mg^{2+} on neural functions in relation to controlling neural activity. However, the relationship between Mg^{2+} and neural functions has not been well understood. Although recent studies indicate that an Mg^{2+} deficient diet has significant health effects, few reports have studied the effect of Mg^{2+} on neural activity [1]. Here we have investigated the effect of low concentrations of extracellular Mg^{2+} on membrane potential using flow cytometry, and on the intracellular Ca^{2+} concentration using a confocal laser microscope.

Figure 1 shows the Mg^{2+} dependence on the membrane potential of cortical neurons. Oxyonol dye DiBAC₄(3) was used for the measurements. The results indicate that a low Mg^{2+} concentration depolarizes the membrane potential depending on the reduction in the extracellular Mg^{2+} concentration below 2 mM [2, 3]. The developmental effect of Mg^{2+} was significant at 12 days in vitro (DIV), and could be observed at a concentration of less than 0.7 mM (Fig. 2) [2, 3].

The same type of Mg^{2+} dependence was observed in hippocampal neurons. However, the responses of cortical and hippocampal neurons to a low Mg^{2+} concentration differed during the developmental period. The results indicate that hippocampal neurons are more sensitive to Mg^{2+} than cortical neurons. This may originate in the difference in the receptor distribution in those regions [3]. Further investigation is needed to understand the mechanisms of the Mg^{2+} effect on neural activity.

[1] K.Torimitsu, N. Kasai, and Y. Furukawa, *Clin. Calcium* **14** (2004) 26.

[2] Y. Furukawa and K. Torimitsu, *JJSMgR* **27** (2008) 75.

[3] Y. Furukawa, N. Kasai, and K. Torimitsu, *Magnes. Res.* **22** (2009) 174S.

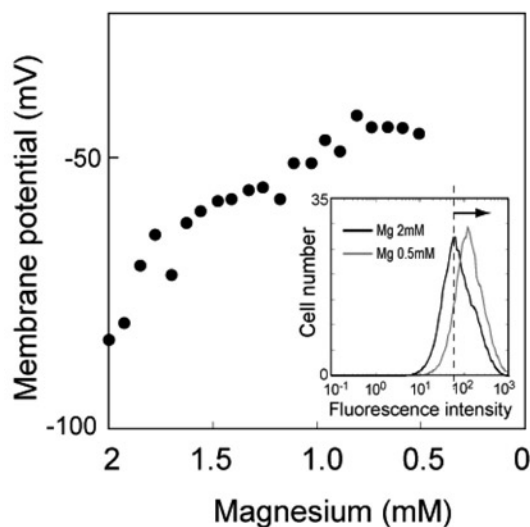


Fig. 1. Magnesium dependence of membrane potential in cortical neurons.

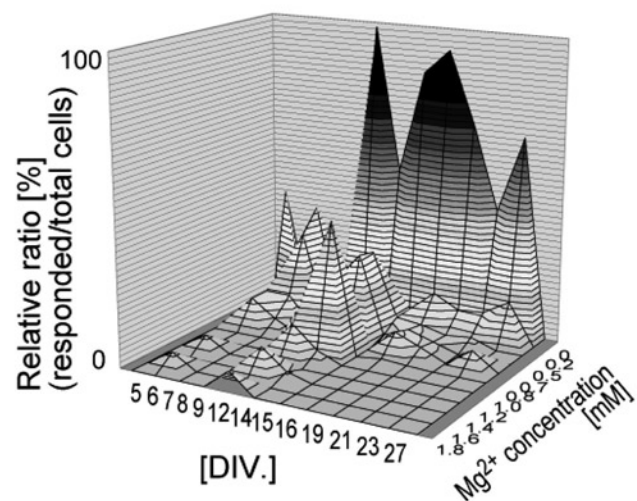


Fig. 2. Developmental effect of magnesium on intracellular Ca^{2+} concentrations.

Fabrication of a Nano-bio Device Using Giant Unilamellar Vesicles

Koji Sumitomo, Arianna McAllister, Yukihiro Tamba*, Youichi Shinozaki,
and Keiichi Torimitsu

Materials Science Laboratory, *Suzuka Nat. Coll. Tech.

To fabricate a nano-bio device that functions with membrane proteins, we are trying to form micron-scale wells covered with a lipid bilayer on a Si substrate [1]. The membrane proteins in the suspended membrane will be able to function as well as membrane proteins *in vivo*. In this study, we used giant unilamellar vesicles (GUVs) several tens of microns in diameter to form a lipid bilayer suspended over the wells.

GUVs have been studied as a simplified cell membrane model. Figure 1 shows a functional analysis of ion channels (gramicidin A) arranged into a GUV lipid membrane based on an analysis of changes in fluorescent intensity. The GUVs' internal environment includes the fluorescent probe (pyranine), which changes its emission intensity with pH. When the environment outside the GUVs is changed (pH is increased), the cations pass through the ion channels and cancel out the concentration gradient between the inside and outside of the GUVs. The increase in the pH of the GUVs with time is clearly shown.

Then, the GUVs were ruptured over the wells which were fabricated on the Si substrate using photolithography. The aperture of the wells has an overhang shape that was formed by selectively etching the Si substrate below the SiO₂ layer. The wells were loaded with fluorescent probes and sealed with a lipid bilayer. Excess probes were rinsed out. Figure 2 shows that the fluorescent probes are trapped in the wells (*b*), although several holes around the patch are unfilled (*a*). The overhang shape improves the probability of the confinement of the fluorescent probes in the wells because the suspended lipid bilayer is prevented from falling into the wells. The fluorescence from the probes confined in the wells remains unchanged for one hour or more. This indicates that the probes remain stably in the wells without flowing out. When we changed the pH outside the wells, we could analyze the function of the ion channels in the suspended lipid bilayer, as in Fig. 1. We show that micron-scale wells for the functional analysis of membrane proteins are formed on the Si substrate.

The transport of ions through the ion channels will be analyzed by both the fluorescent intensity change and the ion current, which will be collected by an electrode embedded in the wells. This constitutes a major step toward the fabrication of nano-bio devices.

[1] Y. Shinozaki et al., Appl. Phys. Express **3** (2010) 027002.

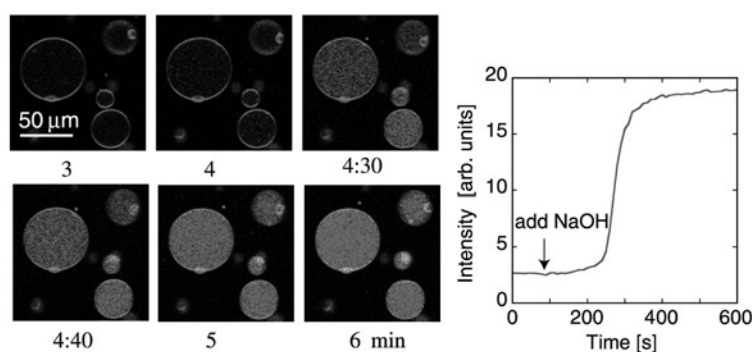


Fig. 1. Functional analysis of ion channels on GUVs (change of fluorescent intensity).

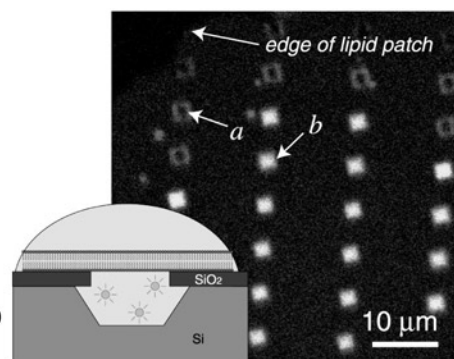


Fig. 2. Sealing of micron-scale wells on a Si substrate with a lipid bilayer.

Design of an LSI Chip for a Bio-machine Interface in 0.18 μm CMOS Technology

Akiyoshi Shimada, Masaya Yamaguchi*, Nobuhiko Nakano*, and Keiichi Torimitsu
Materials Science Laboratory, *Keio University

Brain-machine interfaces that link the brain and the external world have been developed in the neuroscience and medical fields. Most of these interfaces are designed for one-way communication; however we have developed an interface that makes two-way communication possible through a microelectrode array (MEA)[1]. The electrical stimulation of the brain and neural activity measurement are important in relation to this communication, as is the interpretation of information in the brain. Furthermore, an unwired and miniaturized device is desirable in terms of reducing the stress induced when the device is worn on the body. In this study, we have developed 16-ch preamplifiers with multi-channel stimulation circuits on a 2.5 mm \times 1.4 mm LSI chip using a 0.18 μm CMOS process [2].

Figure 1 shows the three main components of this LSI chip: a stimulation block, a measurement block and a mode change block. The stimulation block can produce a 16 ch 4-bit parallel arbitrary waveform by combining 10 μs -wide pluses for electrical stimulation. The measurement block has 16 ch pre-amplifiers, and a multiplexer to combine 16 ch neural signals into one signal at a sampling rate of 40 kS/s. The mode change block switches between the stimulation and measurement blocks when it receives a control signal generated by the stimulation block. Figure 2 shows the neural activity of dissociated rat cortical neurons on the MEA with and without stimulation. A few tens of milliseconds after applying three stimulation pulses to one electrode, neural activity was observed with a different electrode.

We will unwire the input and output between this LSI chip and the external unit to improve the portability of the device as a brain-machine interface.

[1] A. Shimada et al., SFN 2008, Washington, D.C. U.S.A. (Nov. 2008).

[2] M. Yamaguchi et al., Jpn. J. Appl. Phys. Accepted.

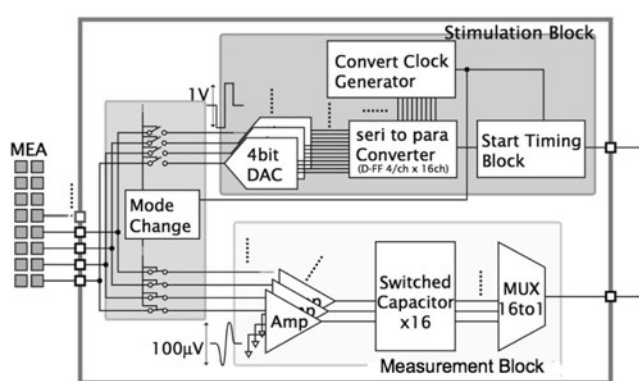


Fig. 1. Circuit diagram of LSI chip designed as brain-machine interface.

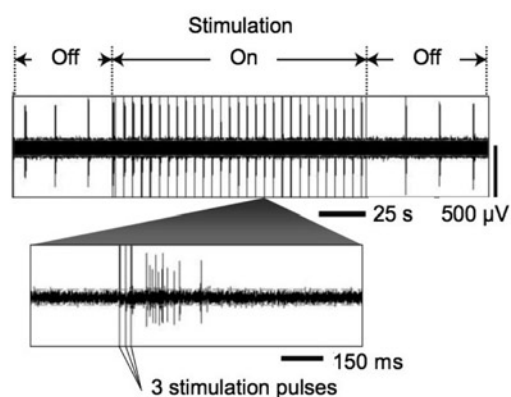


Fig. 2. Neural activity evoked by 3 stimulation pulses.

Si Nanowire Ion-sensitive Field-effect Transistors with a Shared Floating Gate

Katsuhiko Nishiguchi, Toru Yamaguchi, and Akira Fujiwara
Physical Science Laboratory

Ion-sensitive field-effect transistors (ISFETs) are one of the most powerful tools for biotechnology and molecular engineering because they promise high integrability, good miniaturization, and high-speed sensing. More interestingly and importantly, nanoscale ISFETs have sensitivity high enough to detect single electrons at room temperature [1]. On the other hand, a serious issue with ISFETs, which are usually used in ionized and/or charged impurities distributed randomly in a liquid, is background noise. The background noise disturbs the precise detection of small amounts of material, which hinders precise molecular detection. In this study, in an attempt to distinguish a target signal from background noise, we fabricated nanoscale Si-based ISFETs, which are arrayed in parallel and share one floating gate [2].

The ISFET's channels with a constriction part were patterned on a silicon-on-insulator (SOI) wafer (Fig. 1). A subsequent oxidation process shrunk the constriction of the channel, which gives ISFETs high charge sensitivity with single-electron resolution [1]. Au and Ti wires were formed simultaneously on three constrictions by a well-aligned lift-off process using electron-beam lithography. As a substance for detection, we used octadecane thiol (ODT) solved in a tetrahydrofuran (THF). THF with an ODT was dripped onto the ISFETs with a dropper and the characteristics of the current, I_1 , I_2 , I_3 , and I_4 , flowing through the four constrictions in one device were measured.

After complete evaporation of the THF droplet, current characteristics as a function of back-gate voltage shifted according to the concentration of ODT. This means that the fabricated devices work as an ISFET to detect negatively charged ODT on the devices.

Next, we monitored I_1 , I_2 , I_3 , and I_4 in real time when THF with an ODT was supplied (Fig. 2). Although all curves seem to change individually, I_1 , I_2 , and I_3 show mutually synchronized step-wise changes as indicated by arrows, whereas I_4 changes individually. This means that the Au wire covering the channels for I_2 , I_3 , and I_4 is covered with ODT and therefore gives those synchronized changes due to its capacitive coupling to the channels. That is, although each curve individually has background noise or current caused by the THF, ODT, and FETs themselves, real-time monitoring of I_1 , I_2 , I_3 , and I_4 allows us to make a distinction between such background noise and an effect caused by materials attached to the Au wire. The presented scheme is promising for a noise-robust sensor.

[1] K. Nishiguchi, *Jpn. J. Appl. Phys.* **47** (2008) 8305.

[2] K. Nishiguchi, *Appl. Phys. Lett.* **94** (2009) 163106.

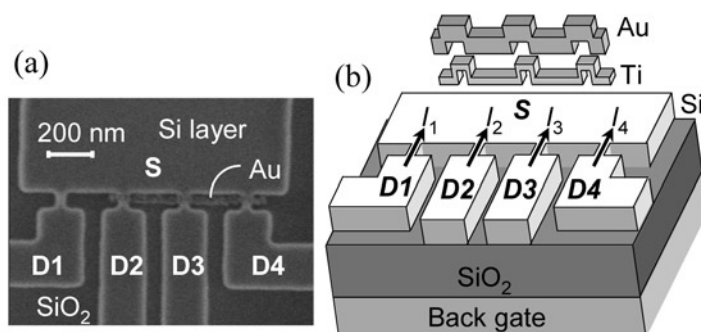


Fig. 1. Device structure of the ISFETs with a shared floating gate. (a) Scanning electron microscope. (b) schematic view.

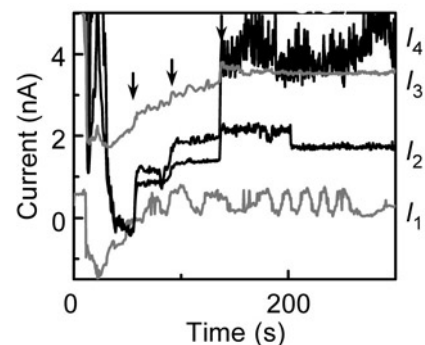


Fig. 2. Change in current flowing through ISFETs when the THF with ODT was supplied.

Tunneling Spectroscopy of Electron Subbands in Thin SOI-MOSFETs

Jin-ichiro Noborisaka, Katsuhiko Nishiguchi, Hiroyuki Kageshima,
Yukinori Ono, and Akira Fujiwara
Physical Science Laboratory

Complementary metal-oxide-semiconductor (CMOS) technology is now approaching the physical limit of scaling where quantum mechanical effects manifest due to the reduction of device size. On the other hand, several new devices are being explored to add functionalities based on quantum effects to silicon devices [1, 2]. Therefore, it is important to understand and control the quantum confinement effect to extend the functionality of silicon devices. Here, we report direct observation of electron subbands in thin silicon-on-insulator (SOI) metal-oxide-semiconductor field-effect transistors (MOSFETs) by tunneling spectroscopy [3].

The observation of subbands was carried out in SOI-MOSFETs with 2-nm-thick tunneling gate oxide [Fig. 1]. Figure 2(a) shows the tunneling current (I_{LG}) and the derivative (dI_{LG}/dV_{LG}) taken at 20 K for a sample with t_{SOI} of 25 nm. Small peaks can be seen when $V_{LG} < 0$. These characteristics are also seen for a device with a t_{SOI} of 10 nm [Fig. 2(b)]. The appearance of these peaks only for negative biases, which causes electron injection into the channel, and their t_{SOI} dependence strongly indicate that they originate from the DOS structure of the thin SOI channel. To understand the observed structures quantitatively, we calculated the energies of the electron subbands in an SOI well for various electric field strengths. We found that the V_{LG} at which the peaks appeared in the experiments is reasonably reproduced by the subband edge of the fourfold valley [Fig. 3(a), (b)]. This is because tunneling current is proportional to the DOS, and the magnitude of the DOS for four-fold valleys is larger than that for two-fold ones, therefore, four-fold valley subbands were clearly detected. We showed clear evidence for the observation of a series of subband spectra in a structurally confined $SiO_2/Si/SiO_2$ quantum well by tunneling spectroscopy.

- [1] K. Uchida et al., *J. Appl. Phys.* **102** (2007) 074510.
[2] S. Saito et al., *Jpn. J. Appl. Phys.* **45** (2006) 679.
[3] J. Noborisaka et al., *Appl. Phys. Lett.* **96** (2010) 112102.

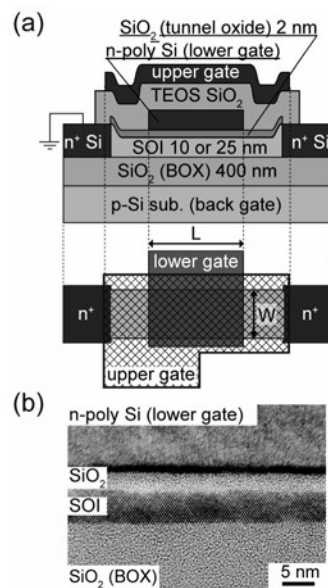


Fig. 1. (a) Schematic view of the device. (b) Transmission electron microscope image.

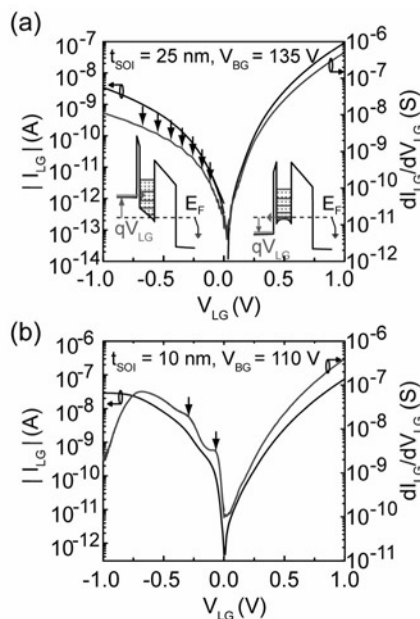


Fig. 2. Tunneling current and conductance. (a) SOI = 25 nm; (b) SOI = 10 nm.

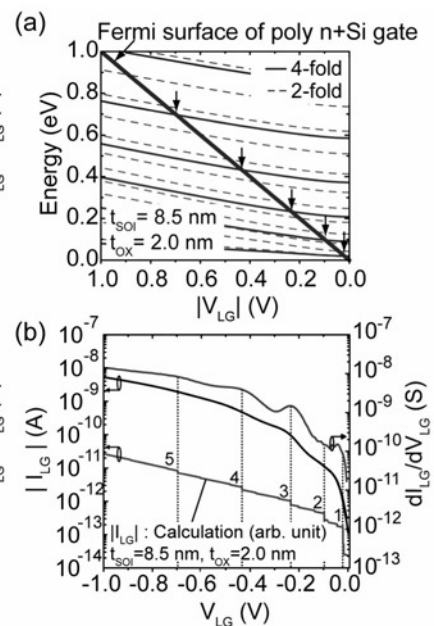


Fig. 3. (a) Calculated subband energies. (b) Comparison between the calculated tunneling current and experimental one.

Two-dimensional Patterning by Using Block Copolymer Self-assembly

Toru Yamaguchi and Hiroshi Yamaguchi
Physical Science Laboratory

Block copolymer lithography has drawn considerable attention as a combined top-down/bottom-up nanopatterning method toward 16-nm-technology nodes and beyond. The most important challenge of its application to nanodevice fabrication is in achieving two-dimensional (2D) patterning by strictly controlling the alignment of the domain interface of the microphase-separated domains of a block copolymer. Here, we demonstrated that a flexibly designable 2D self-assembly of the symmetric poly(styrene-*b*-methylmethacrylate) (PS-*b*-PMMA) (M_n : 36 kg mol⁻¹, lamellar period $L_0=28$ nm) is achieved by graphoepitaxy using a hydrogen silsesquioxane (HSQ) resist pattern as the guide for alignment [1]. The key to success is the combination of the neutralization of the bottom surface and the introduction of an intentionally designed 2D hydrophilic guiding pattern formed by top-down electron-beam lithography (EBL), which leads to vertical orientation and 2D alignment of lamellar domains, respectively [Fig. 1(a)].

For rectangular confinement, vertical lamellar domains with a thickness of $4L_a$ (L_a : average repeating period of the laterally aligned lamellar domains) and with a half-pitch of 16 nm can be forced to bend using right-angled guiding patterns [Fig. 1(b)]. It is noteworthy that these domain structures are formed in a pure block copolymer system, which can be achieved with high flexibility in the domain shape and period in graphoepitaxy of lamellar domains of diblock copolymers. For hexagonal confinement, we have successfully demonstrated that concentric cylindrical domains are formed [Fig. 1(c)]; these domains are characterized by high controllability of the number of layers of the PS or PMMA rings, which is achieved by varying the width of confinement between opposite sides. This precise control of the alignment of lamellar domains can be achieved by first taking full advantage of the bottom-up self-assembly of block copolymers and the top-down fabrication of the alignment guide by using high-precision EBL. We have also confirmed that these bent lamellae and concentric cylinders were successfully transferred to a semiconductor substrate with a 16-nm half-pitch resolution [Fig. 1(d)]. We are convinced that our method increases the applicability of block copolymer lithography to nanodevice fabrication, as the size scale is beyond the reach of the state-of-art top-down technology.

[1] T. Yamaguchi and H. Yamaguchi, *Adv. Mater.* **20** (2008) 1684.

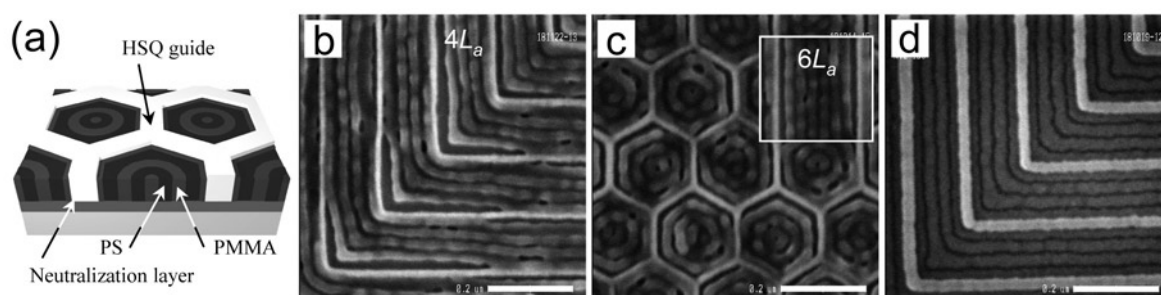


Fig. 1. (a) Schematic diagram of the self-assembled structure in a hexagonal confinement. (b, c) Top-down Scanning Electron Microscope (SEM) images of retained PS domains after the removal of the PMMA domains in (b) rectangular and (c) hexagonal confinements. (d) Top-down SEM image of etched patterns. All scale bars are 200 nm.

Optical Tuning of Coupled Nanomechanical Resonators

Hajime Okamoto, Koji Onomitsu, and Hiroshi Yamaguchi
Physical Science Laboratory

Coupled nanomechanical resonators have recently become the focus of research because they allow the study of interesting physical phenomena, such as synchronization and mode localization[1,2]. They also enable new applications in sensors using the dynamics of the coupled system[3]. The coupling efficiency is determined by the eigenfrequency difference in the resonators. Therefore, frequency tuning is important and desired to control the vibrational coupling. Here, we demonstrate the controlled coupling in nanomechanical resonators by using photothermal stress. By this method, perfect vibrational coupling was realized[4].

The nanomechanical system has two doubly-clamped beams of 40- μm length, 10- μm width, and 0.8- μm thickness (Fig. 1). The beams consist of top Au gates, AlGaAs/GaAs superlattice, n -GaAs, and i -GaAs layers. The two beams are mechanically coupled through an etching overhang. Each beam can be actuated separately by the piezoelectric effect by applying an a.c. voltage between the gate and the n -GaAs layer. The frequency response of the mechanical vibration was detected using a He:Ne laser via optical interferometry (Fig. 1). The eigenfrequency of the beams was tuned by adjusting the laser power. These measurements were performed in a vacuum at room temperature.

Figure 2 shows the laser power dependence of the resonance spectra of Beam 2 measured whilst actuating Beam 1. Two coupled vibrational modes are found around the natural frequency: the nearly symmetric and anti-symmetric vibration for the lower- and higher-frequency, respectively. The coupling efficiency between the beams can be controlled by adjusting the laser power (P). Photo-induced thermal stress modifies the eigenfrequency of the beam with changing its spring constant. Increasing P reduces the eigenfrequency difference between the two beams, therefore enhancing the coupling efficiency. The frequency difference between the two coupled modes decreases with increasing P and is minimized at $P = 64 \mu\text{W}$ (Fig. 2). At this laser power, the coupling is maximized and purely symmetric and anti-symmetric vibration is realized. For $P > 64 \mu\text{W}$, the frequency difference again increases with P increases, i.e., the coupled beams are optically detuned. The realization of the perfectly tunable coupled nanomechanical resonators will offer the opportunity for their high-sensitive sensing applications and for the study of the dynamics of coupled systems.

- [1] S. Shim et al., Science **316** (2007) 95.
- [2] C. Pierre, J. Sound Vib. **139** (1990) 111.
- [3] M. Spletzer et al., Appl. Phys. Lett. **88** (2006) 254102.
- [4] H. Okamoto et al., Appl. Phys. Express **2** (2009) 062202.

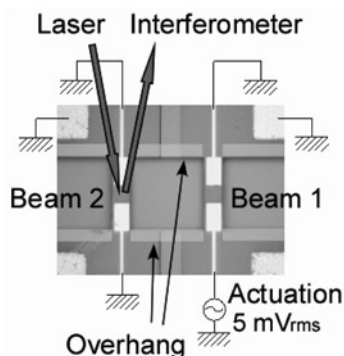


Fig. 1. Microscope image of the coupled resonators and an illustration of the measurement setup.

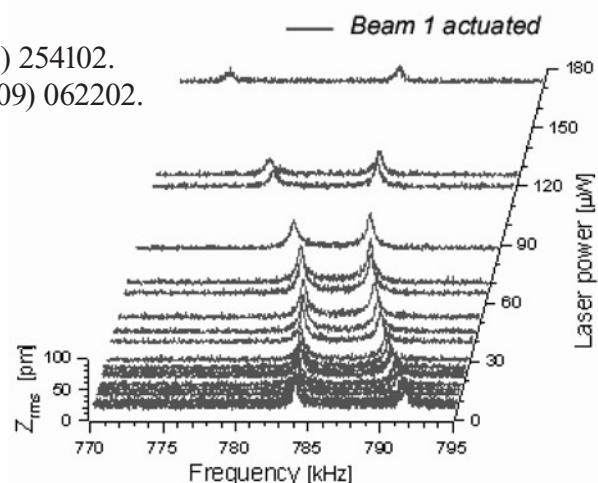


Fig. 2. Laser power dependence of the resonance spectra of the coupled modes.

Intrinsic Gap and Exciton Condensation in the $\nu_T = 1$ Bilayer System

Paula Giudici, Koji Muraki, Norio Kumada, and Toshimasa Fujisawa
Physical Science Laboratory

A system comprising two layers of two-dimensional electron systems (2DES) closely separated at a distance of 20-30 nm, termed a bilayer electron system, exhibits unusual properties not seen in single-layer systems. In particular, for a system where macroscopically degenerate discrete levels (Landau levels), formed in each layer by a magnetic field applied perpendicular to the 2D plane, are half filled by electrons (i.e., total filling factor $\nu_T = 1$) and the interlayer distance d is small enough so that the interlayer interaction is strong, many interesting phenomena, including dissipationless flow of electrical current oppositely directed in the two layers suggestive of excitonic superfluidity [1], have been reported. On the other hand, when d is large enough so that the two layers behave independently, the system exhibits a metallic behavior, which is believed to reflect the Fermi surface formed by composite particles consisting of electrons and magnetic flux quanta.

The nature of the quantum phase transition between these largely dissimilar quantum states has long been a subject of both theoretical and experimental interest. However, in a recent study [2] we have shown that, in the standard experimental conditions, where a GaAs double quantum well is subjected to a perpendicular magnetic field, the metallic phase is not fully spin polarized and, as a result, the experimentally observed transition is governed by the Zeeman energy, which results in a first order transition with different nature than that of a quantum phase transition expected for an ideal spinless system. In this study, by tilting the magnetic field with respect to the sample normal and thereby enhancing the Zeeman energy, we investigated the nature of the intrinsic phase transition without any spin effects [3]. As the Zeeman energy is increased, the energy gap of the excitonic phase saturates at a value (intrinsic gap) that depends solely on the ratio between the interlayer distance d and the in-plane electron distance l_B (Fig. 1) and its amplitude coincides with twice the energy difference between the two states (Fig. 2). These results suggest that this phase transition is of second order and the condensate is formed from the metallic state through exciton formation.

[1] M. Kellogg et al., Phys. Rev. Lett. **93** (2004) 036801.

[2] P. Giudici, K. Muraki, N. Kumada, Y. Hirayama, and T. Fujisawa, Phys. Rev. Lett. **100** (2008) 106803.

[3] P. Giudici, K. Muraki, N. Kumada, and T. Fujisawa, Phys. Rev. Lett. **104** (2010) 056802.

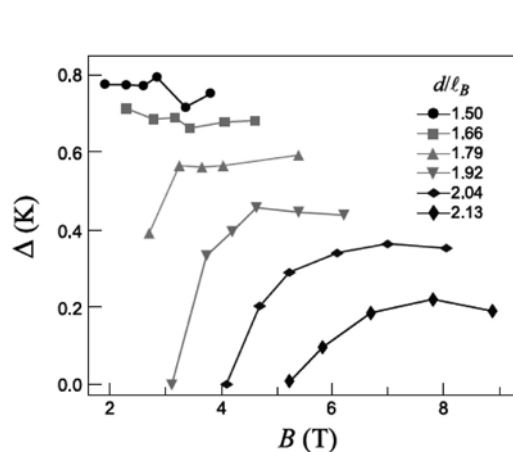


Fig. 1. Energy gap of the excitonic phase at different d/l_B plotted as a function of the total magnetic field.

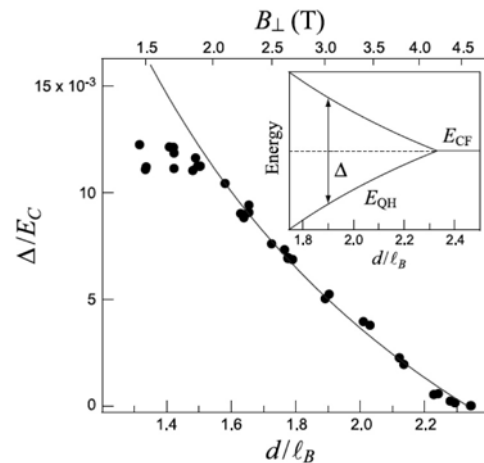


Fig. 2. Intrinsic gap vs d/l_B and comparison with twice the energy difference (solid line).

Fano-Kondo Effect in a Side-coupled Double Quantum Dot

Satoshi Sasaki and Hiroyuki Tamura
Physical Science Laboratory

Large tunability of electronic states in semiconductor quantum dot (QD) systems has unveiled rich quantum transport phenomena such as the Kondo effect and Fano resonances. The Kondo effect arises from spin singlet formation between the localized magnetic moment in the QD and the conduction electrons in the reservoirs, and drastically modifies the transport characteristics of the QD at low temperature. When a second QD (dot 2) is tunnel-coupled to the side of the first QD (dot 1) exhibiting the Kondo effect, as schematically shown in Fig.1, the inter-dot spin singlet formation is expected to suppress the Kondo effect. Although a large number of theoretical studies exist on such a side-coupled double QD, very few experiments have been reported so far. On the other hand, Fano effect arises from interference between continuum and a resonant channel. Ratio of the transmission amplitudes via the two channels determines the Fano resonance wave form ranging from an asymmetric peak to a dip.

In this work, we measure low temperature transport characteristics of the side-coupled double QD fabricated from GaAs/AlGaAs two dimensional electron system, and discuss novel Fano-Kondo interplay [1]. Figure 2 shows a grey-scale plot of the conductance as functions of the plunger gate voltages, V_1 and V_2 , measured with a standard lock-in method at 41 mK. Three strong Coulomb peaks are observed when the electron number in dot 1, N_1 , changes by one. Conductance between the two Coulomb peaks marked with a triangle is enhanced by the Kondo effect where N_1 is odd. Inter-dot Coulomb interaction is revealed as jumps in the Coulomb peak positions whenever the electron number in dot 2, N_2 , changes by one, forming a well-known honeycomb stability diagram. We observe conductance maxima at the upper valley (white arrow) and minima at the lower valley (black circle) when N_2 changes by one. Detailed temperature and magnetic field dependence measurement of these features lead us to conclude that they are Fano resonances where the Kondo effect (cotunneling) in dot 1 plays a role of continuum. These features are qualitatively reproduced by theoretical calculations [2].

[1] S. Sasaki et al., Phys. Rev. Lett. **103** (2009) 266806.

[2] H. Tamura and S. Sasaki, Physica E **42** (2010) 864.

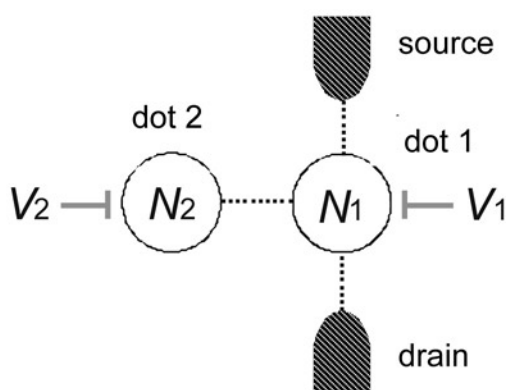


Fig. 1. Schematic diagram of the side-coupled double quantum dot structure.

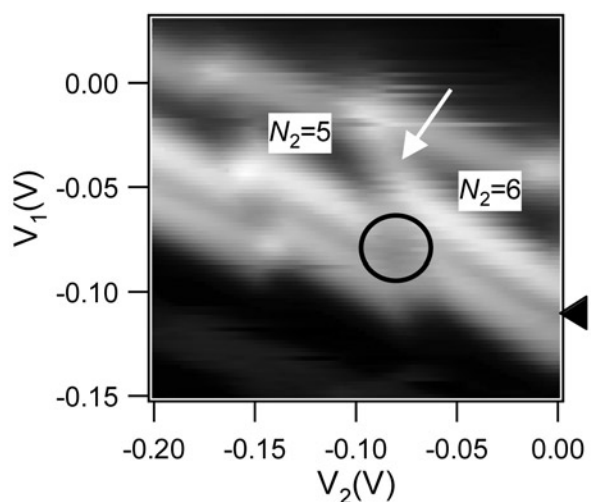


Fig. 2. Observed conductance as functions of the plunger gate voltages. White corresponds to high conductance.

Multiple Two-qubit Operations Using Semiconductor Coupled Charge Qubits

Takeshi Ota, Gou Shinkai*, Toshiaki Hayashi, and Toshimasa Fujisawa*
Physical Science Laboratory, *Tokyo Institute of Technology

Two-qubit unitary operations are key ingredients for performing quantum algorithms and correlating multiple qubits. Typical operations, such as controlled-rotation (CROT), which rotates the target qubit state conditionally on the control qubit state, and SWAP, which swaps quantum states of the two qubits, have been demonstrated using superconductor charge qubits and semiconductor spin qubits[1, 2]. However usually one type of operations is realized depending on the type of coupling (Ising, Heisenberg, etc.). Although other operations can in principle be designed in combination with some one-qubit operations, simple sequences for shorter operation time or a smaller number of steps have been desired to maintain the coherency of the system.

In this work, using coupled semiconductor charge qubits consisting of two sets of coupled double quantum dots (DQD), we fabricated two-qubit device in which two spatially separated electrons in the two qubits change their locations coherently and collectively (the correlated coherent oscillations) and two-qubit operations such as CROT, SWAP can be performed in a single step[3]. Figure 1 shows a scanning electron micrograph (SEM) of the two-qubit device. The two qubits with individual source and drain electrodes are electrically isolated, and thus independent currents can be measured simultaneously. All qubit parameters can be controlled by 11 gate voltages. By applying high-frequency voltage pulse to first qubit and measuring the current, coherent oscillation demonstrating the superposition of the charge states $|0\rangle$ and $|1\rangle$ is observed. Here, $|0\rangle$ and $|1\rangle$ represent the location of the charge in the right and left dot, respectively. Due to the electrostatic coupling between the two qubits, the coherent oscillation of the first qubit is strongly influenced by the charge states of the second qubit. Figure 2 shows the demonstration of the CROT operation of the first qubit using the second qubit as a control qubit. Figure 3(a) shows the correlated coherent oscillations in which SWAP operation is performed.

This work was partly supported by SCOPE from the Ministry of Internal Affairs and Communications of Japan.

- [1] T. Yamamoto et al., Nature **425** (2003) 941.
[2] J. R. Petta et al., Science **309** (2005) 2180.
[3] G. Shinkai et al., Phys. Rev. Lett. **103** (2009) 056802.

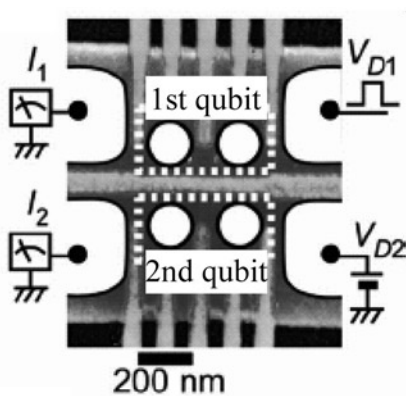


Fig. 1. Two-qubit device using coupled semiconductor double quantum dots.

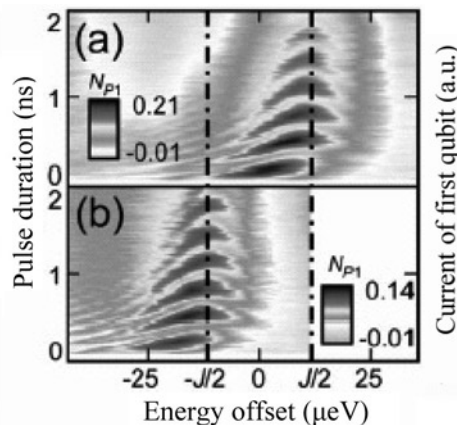


Fig. 2. Coherent oscillations of the first qubit representing CROT operation. The oscillations (a) and (b) correspond to the case that the second qubit is $|1\rangle$ and $|0\rangle$, respectively.

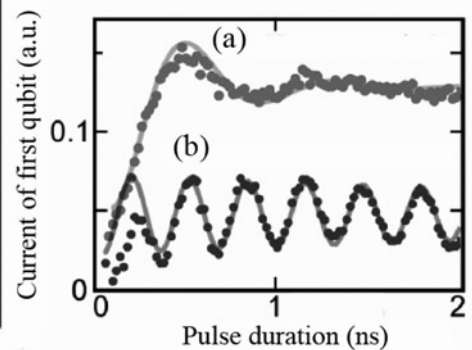


Fig. 3. (a) Correlated coherent oscillations of the first qubit. The oscillations (b) correspond to those shown in Fig. 2.

Theory of Quantum Dynamics During a Qubit Readout Process with a Josephson Bifurcation Amplifier

Hayato Nakano, Kosuke Kakuyanagi, Shiro Saito, Kouichi Semba, and Hideaki Takayanagi*
Physical Science Laboratory, *Tokyo University of Science

The readout of a qubit state is a typical indirect quantum measurement that is performed with a probe. We report here our successful theoretical analysis of a superconducting qubit readout with a Josephson bifurcation amplifier (JBA) as the probe. We also use this readout method in our experiments.

JBA is a non-linear oscillator, which has two resonance modes (high-amplitude mode E state, and low-amplitude mode G state). Small changes in operational parameters (driving frequency, driving amplitude, etc.) determine which mode is realized. When we make a JBA interact with a qubit, the resulting JBA state reflects a small change in the effective operational conditions depending on the qubit state. So, we can readout the qubit state (microscopic information) as the realized JBA state (macroscopic information) [1]. This constitutes a form of quantum signal amplification. The JBA readout method is suitable for quantum processing because it has almost no detrimental effect on the post-measurement qubit state. The readout process is certainly the quantum time-evolution (quantum dynamics) of a qubit-JBA coupled system. We have clarified the process theoretically. In particular, we have shown how a superposed qubit is projected into one of the measurement basis states probabilistically during this readout process [2].

As the driving force is increased, the interaction between the qubit and the JBA gradually increases, and the unitary evolution makes the coupled system become an entangled state consisting of two qubit-JBA correlated states ($0 < t < \tau_1$; see figures below). In one of them the qubit is in the excited (e) state, and the JBA is in the G state. In the other, the qubit is in the ground (g) state, and the JBA is in the G' . As the driving force is further increased, the g - G' pair starts to transit to g - E . At this point, the decoherence in the JBA destroys the entanglement ($t \sim \tau_2$). In due course, the coupled system becomes a mixture consisting of an e - G and g - E pair. This means that the coupled system is now ($t \sim \tau_3$) one of the two possible states although we do not know which is realized until we perform a measurement. By judging whether the JBA state is G or E with a usual classical measurement, we can know into which state (g or e) the qubit is projected.

[1] I. Siddiqi et al., Phys. Rev. Lett. **93** (2004) 207002.

[2] H. Nakano, S. Saito, K. Semba, and H. Takayanagi, Phys. Rev. Lett. **102** (2009) 257003.

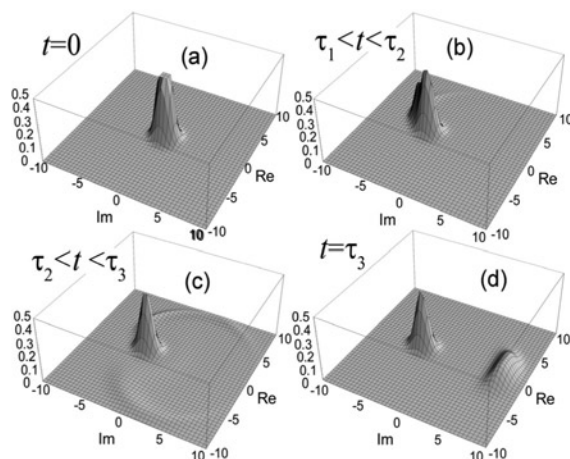


Fig. 1. Time-evolution of JBA (a) \rightarrow (b) \rightarrow (c) \rightarrow (d) (Q-representation).

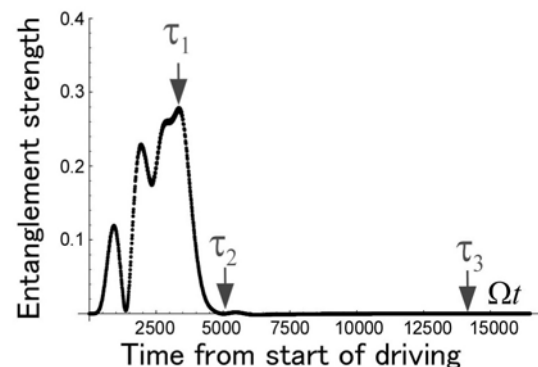


Fig. 2. Time variation of entanglement strength between qubit and JBA.

Experimentally Realizable Controlled-NOT Gate in a Flux-qubit / Resonator System

Shiro Saito, Todd Tilma*, Simon J. Devitt*, Kae Nemoto*, and Kouichi Semba
Physical Science Laboratory, *National Institute of Informatics

Superconducting qubits have attracted increasing interest in the context of quantum computing and quantum information processing [1]. We are focusing on a superconducting flux qubit/resonator system [see Fig. 1(a)] where the resonator works as a quantum bus (qubus). Using the qubus concept we can perform any two-qubit operation between any two qubits that are coupled to the quantum bus without using multiple swap gates, which are required in other systems that use direct qubit-qubit coupling. We present an experimentally realizable microwave pulse sequence that effects the controlled-NOT (C-NOT) gate operation in a qubit/resonator system [2]. From numerical simulations, we obtained a process fidelity F_p [3] of 98.8 % (98.0 %) for a two-(three-)qubit/resonator system under ideal conditions.

Figure 1(a) is a schematic of our system. Each qubit couples to the resonator through a mutual inductance M . Because of the fixed coupling, the qubit transition frequency depends slightly on the resonator state. We utilize this frequency difference to realize the C-NOT gate in cooperation with a two-photon blue side band (BSB) transition, which can create an entanglement between the control qubit and the resonator. Figure 1(b) shows a basic operational sequence of pulses on our two-qubit/resonator system. The pulse characteristics are represented by a frequency (C: carrier frequency, BSB: BSB frequency), a length ($\pi/2$, π) and a phase (0, π , φ) from the top to the bottom. We obtained an F_p of 98.8 % by optimizing the free evolution time T and the phase of the second BSB pulse φ . Here we set the frequencies of the control, target qubit and resonator at 6, 5 and 10 GHz, respectively, and the coupling between the qubit and the resonator at 0.1 GHz. Moreover, we obtained a high F_p of 98.0 % even when we added a third qubit with a frequency of 7 GHz, which means that our proposal is scalable. The total gate time is 200 ns, which is much shorter than the coherence time of a flux qubit (4 μ s). We estimated F_p under decoherence (see Fig. 2). We obtained an F_p of 90.3 % under the best conditions yet achieved experimentally: $Q=10^6$ and $\Gamma_1=\Gamma_2=0.25$ MHz. Even with this realistic decoherence model, F_p still exceeds 90 %, showing that our gate remains robust against this type of loss.

This work was supported by KAKENHI.

[1] J. Clarke and F. K. Wilhelm, *Nature* **453** (2008) 1031.

[2] S. Saito, T. Tilma, S. J. Devitt, K. Nemoto, and K. Semba, *Phys. Rev. B* **80** (2009) 224509.

[3] I. L. Chuang and M. A. Nielsen, *J. Mod. Opt.* **44** (1997) 2455.

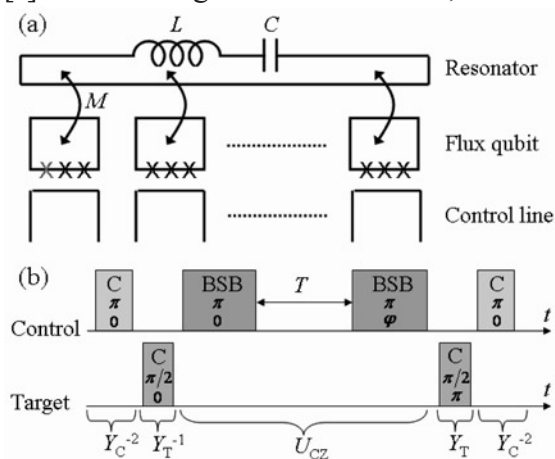


Fig. 1. (a) Superconducting flux-qubit/resonator system.
(b) Pulse sequence of C-NOT gate.

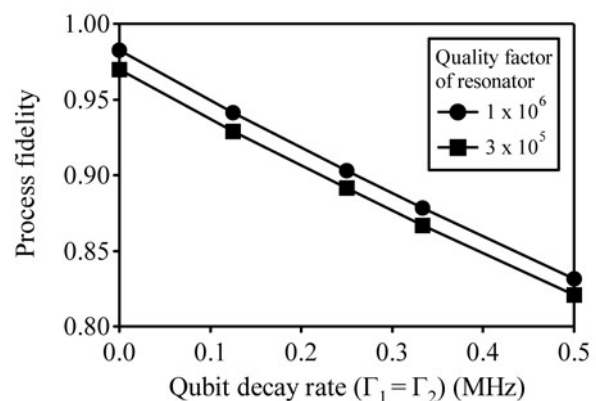


Fig. 2. Process fidelity under decoherence.

Kondo Effect in a Semiconductor Quantum Dot Controlled by Spin Accumulation

Toshiyuki Kobayashi¹, Shoei Tsuruta^{1,2}, Satoshi Sasaki¹, Toshimasa Fujisawa¹,
Yasuhiro Tokura³, and Tatsushi Akazaki^{1,2}

¹Physical Science Laboratory, ²Tokyo University of Science, ³Optical Science Laboratory

The spin of a localized electron embedded in a semiconductor quantum dot interacts with the spins of surrounding conduction electrons to form a spin-singlet coherent quantum many-body state. The state is known as the Kondo effect, which changes the state by temperature, electric field, and magnetic field. Since both the localized and conduction electrons play important roles in forming the Kondo state, the Kondo effect should be suppressed if the conduction electrons are spin-polarized. However, any experimental investigation of the Kondo effect with spin-accumulated conduction electrons had been a challenge owing to the difficulty of generating a 100 % spin-polarized state. We have succeeded in measuring the continuous modulation of the Kondo effect by accumulating only spin-up electrons near a quantum dot using a spin filter of a quantum wire under a high magnetic field whose spin selectivity is more than 90 % [1].

The Kondo effect accompanies the formation of the Kondo density of states (KDOS) at the chemical potential μ of a lead, because the conduction electrons at the Fermi energy interact resonantly with the localized electron (Fig. 1). Since the KDOS moves with μ , changing the μ of just the spin-up electrons by injecting only spin-up electrons from a quantum wire to a quantum dot shifts only the spin-up KDOS and modulates the spin-splitting of the KDOS. The position of the KDOS can be measured as a peak in the differential conductance g_D of a quantum dot (Fig. 2).

[1] T. Kobayashi et al., Phys. Rev. Lett. **104** (2010) 036804.

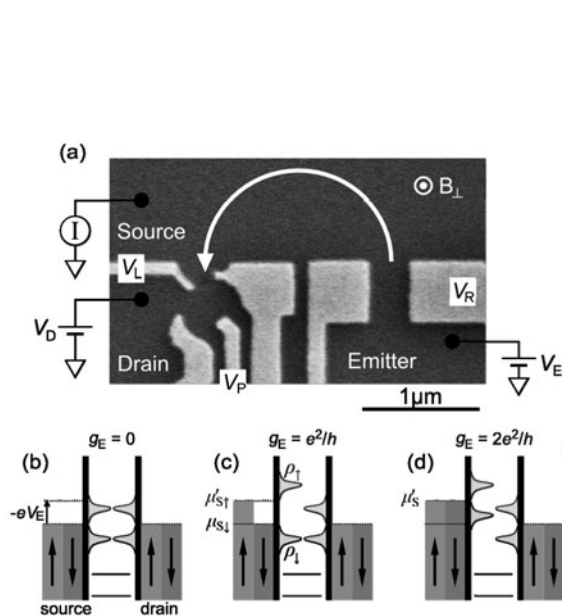


Fig. 1. (a) Scanning electron micrograph of the device and the measurement setup. (b)-(d) Chemical potentials μ and KDOS ρ when the conductance g_E of a quantum wire is fixed at 0, e^2/h , and $2e^2/h$ and V_E is applied.

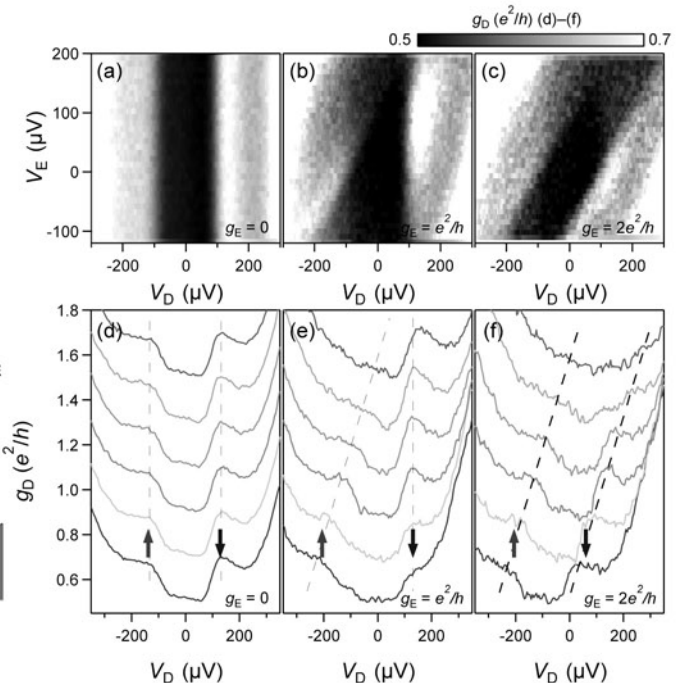


Fig. 2. Conductance peak attributed to the KDOS shifts with V_E . When the conductance g_E of a quantum wire is e^2/h , the μ of a spin-up electron shifts with V_E , which is measured as a shift in the conductance peak.

Generation of Time-bin Entangled Photon Pairs Using Cascaded Second Order Nonlinearity in Single PPLN Waveguide

Myrtille Hunault, Hiroki Takesue, Osamu Tadanaga*, Yoshiki Nishida*, Masaki Asobe*
Optical Science Laboratory, *NTT Photonics Laboratories

Cascaded second-order nonlinearity ($\chi^{(2)}$: $\chi^{(2)}$) process in a single periodically poled lithium niobate (PPLN) waveguide is a well known technique for wavelength conversion in the 1.5- μm band [1]. Recently, this technique has been used in a quantum optics experiment, in which squeezed vacuum pulses were generated [2]. Here, we report the generation of time-bin entangled photon pairs using the $\chi^{(2)}$: $\chi^{(2)}$ process in a single PPLN waveguide.

Figure 1 shows the setup. A 1551.1 nm continuous lightwave was modulated into a pulse train with a 100 ps width and a 500 MHz repetition frequency using an intensity modulator (IM). The pulses were amplified by an erbium-doped fiber amplifier (EDFA), filtered to eliminate amplified spontaneous emission noise from the EDFA, and then launched into a PPLN waveguide. In the PPLN waveguide, the 1.5- μm pump pulse train was converted to a 780-nm pulse train via SHG (second harmonic generation), and simultaneously, the generated 780-nm pulse train worked as a pump for spontaneous parametric down conversion. As a result, we generated sequential time-bin photon pairs [3], whose state is approximately given by $\frac{1}{\sqrt{N}} \sum_{k=1}^N |k\rangle_x |k\rangle_i$. Here, $|k\rangle_z$ denotes the state of a photon in the temporal position k and the mode z ($=s$: signal, or i : idler), and N is the number of pulses for which the phase coherence of the pump is preserved. The output light from the PPLN waveguide was introduced into optical filters, which separated the signal and idler photons. The signal and idler photons were then input into 1-bit delayed interferometers. We can observe a two-photon interference fringe by measuring the coincidence counts between the signal and idler channels while changing the phase of the interferometers.

As shown in the inset of Fig. 1, we observed two-photon interference fringes with visibilities up to as high as 97 %. Thus, we successfully confirmed the generation of high-purity entanglement based on the proposed scheme.

[1] M. H. Chou et al., IEEE Photon. Technol. Lett. **11** (1999) 653.

[2] K. Hirose et al., Phys. Rev. A **80** (2009) 043832.

[3] H. de Riedmatten et al., Phys. Rev. A **69** (2004) 050304(R).

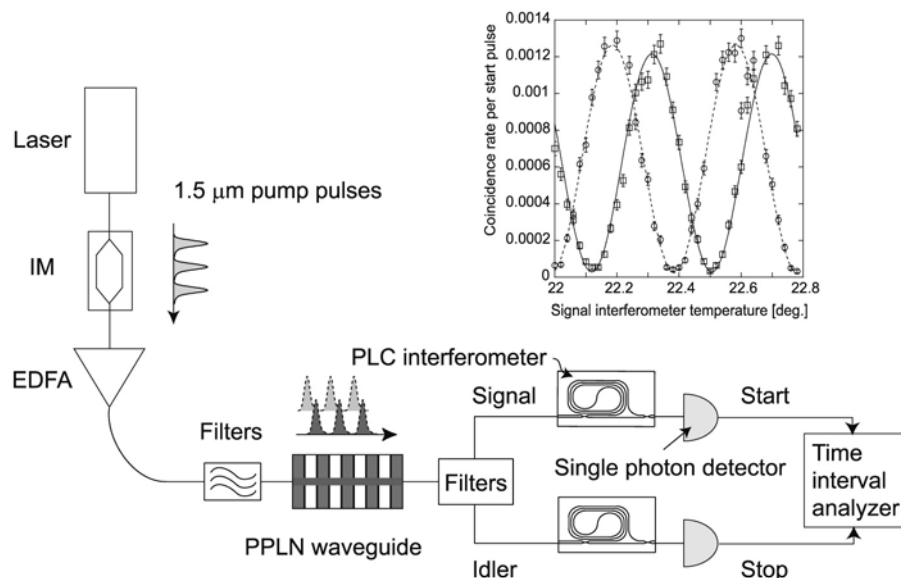


Fig. 1. Experimental setup (inset: two-photon interference fringes).

Numerical Analysis of Cold Fermionic Atoms in an Optical Lattice at Finite Temperatures

Kensuke Inaba and Makoto Yamashita
Optical Science Laboratory

Cold atoms trapped in optical lattices are ideal model systems for investigating the many-body problems which have been studied for many years in condensed matter physics. These controllable systems are thus considered as a quantum simulator. In fact, the quantum phase transition from a metallic state to a Mott insulating state has been successfully realized using fermionic ^{40}K atoms in optical lattices [1]. The antiferro-magnetic (AF) transition in the optical lattice system is a major current concern for condensed matter physicists, because it could provide ways to elucidate the nature of high T_c superconductors. According to the recent rapid progress in cold atom experiments, one can expect the AF phase in optical lattice systems to be observed at lower temperatures in the near future. This naturally motivates us to undertake a detailed theoretical study of the properties of the AF transition in this system. However, there was no reliable theoretical method to investigate this issue, because the trapping potential, which is a characteristic of optical lattice systems, makes the analysis much more complex.

We have investigated the two-component fermionic atoms trapped in a two-dimensional (2D) optical lattice [2]. We extended the self-energy functional approach (SFA), which is known as a powerful numerical tool to analyze strongly correlated electron systems at finite temperatures. However, due to the trapping potential, it has been difficult to investigate realistic optical lattice systems using a conventional SFA algorithm. We solved this difficulty and confirmed that the extended-SFA can be successfully applied to the 2D optical lattice system. The calculated results showed reasonable agreements with the previous experimental and theoretical results [1]. Furthermore, we studied the AF transition in this 2D optical lattice system systematically. As shown in Fig. 1, below the AF transition temperature, the AF ordered region develops from the bottom of the trapping potential where the Mott insulating region appears at certain higher temperatures. Finally, we estimated the AF transition temperature (Fig. 2), and proposed a suitable parameter region for observing the AF ordered phase experimentally.

This work was partly supported by CREST of the Japan Science Technology Agency.

- [1] U. Schneider et al., *Science* **322** (2008) 1520; R. Jordens et al., *Nature* **455** (2008) 204.
[2] K. Inaba and M. Yamashita, submitted to *Phys. Rev. A*.

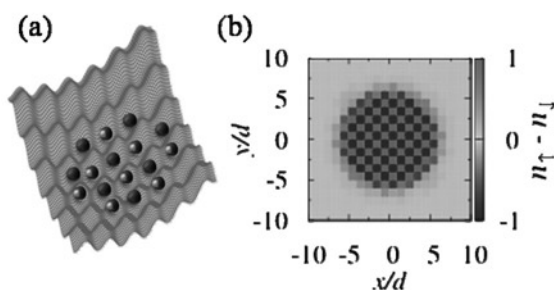


Fig. 1. (a) Schematic diagram of the AF ordered phase of two-component fermions trapped in a 2D optical lattice. (b) Numerical result: Spatial distribution of magnetization below the AF transition temperature.

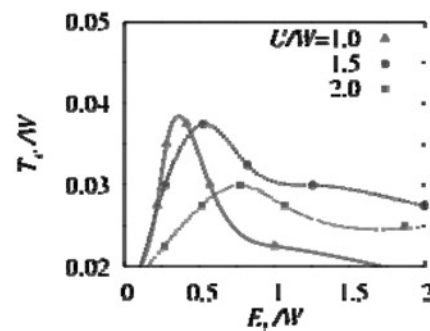


Fig. 2. AF transition temperatures T_c as a function of characteristic energy scale of trapping potential E_t for different interaction strengths U , where energy unit W is the bandwidth.

Trapping Loss Mechanism of Superconducting Atom Chips

Tetsuya Mukai, Christoph Hufnagel, and Fujio Shimizu*

Optical Physics Laboratory,

*The University of Electro-Communications

A stable confinement of neutral atoms in quantum regime is an indispensable technique for realizing quantum gate operations over an atomic system. Trapping atoms with a field of micro-fabricated circuit on chip "atom chip" enables strong trapping confinement with practical resources and it is expected to be a key technology for quantum manipulation of atoms. The first step for developing the atom chip quantum device is overcoming a serious loss problem that is significant in the vicinity of a chip surface. Our approach is employing a superconducting circuit, which is expected to reduce the spin-flip loss rate in many orders of magnitude. So far we have succeeded in trapping atoms with a superconducting circuit with persistent current [1] and demonstrated an order improvement in trapping stability. However, our experimental results also suggested that the trapping loss mechanism of superconducting atom chip is not the same as that of conventional atom chips. In this year we studied and clarified the trapping loss mechanism of superconducting atom chip [2].

At first we investigated the current distribution in a superconducting wire by measuring the trap height over applied bias field (Fig. 1). By comparing with the calculated trap height with and without magnetic fluxes, the experimental result clearly suggested that magnetic fluxes were penetrating into the superconducting wire.

Secondly we analyzed the experimentally obtained trapping loss rate as a function of trap heights (Fig. 2). The trapping loss rate shows specific curve when the data was taken with the same persistent current, but after washing out the current and re-introducing the persistent current, the loss rate shows a different curve. With these experimental results, we came to understand that the penetrated magnetic fluxes with dendritic pattern locally modified the trapping potential and introduced a spin flip transition at zero field point. The existence of dendritic magnetic fluxes was also proved by an experiment with a novel trap with a superconducting disc [3].

This research was partly supported by CREST of Japan Science and Technology Agency and KAKENHI.

[1] T. Mukai, C. Hufnagel et al., Phys. Rev. Lett. **98** (2007) 260407.

[2] C. Hufnagel, T. Mukai, and F. Shimizu, Phys. Rev. A **79** (2009) 053641.

[3] F. Shimizu, C. Hufnagel, and T. Mukai, Phys. Rev. Lett. **103** (2009) 253002.

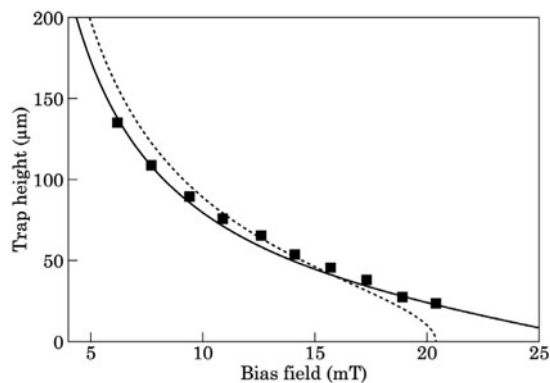


Fig. 1. Trap height over applied bias magnetic field. The filled squares represent the experimental data and solid (dotted) curve represents a calculation with (without) magnetic flux penetration.

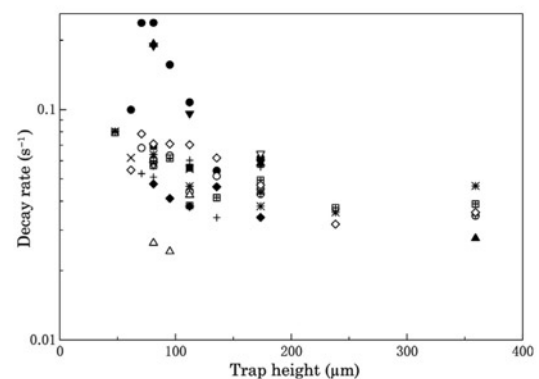


Fig. 2. Decay rate over several trap heights. Different marks represent the data taken on the different days. Persistent current was introduced several times on each day.

Ultrafast Dynamics of Coherent Phonons in P-type Si Driven by Sub-10-fs Laser Pulses

Keiko Kato, Atsushi Ishizawa, Katsuya Oguri, Hideki Gotoh, and Hidetoshi Nakano
Optical Science Laboratory

Coherent phonons are the in-phase lattice vibrations driven by the ultrashort laser pulses whose duration is shorter than the oscillatory period. In contrast to frequency-domain approaches, such as Raman spectroscopy or infrared-active spectroscopy, the observation of coherent phonons provides time-domain information about the lattice vibrations.

For Si, which is the fundamental semiconductor, the Raman spectrum is modified by p-type doping, reflecting the asymmetric shape of the valence band in k -space [1]. To study the electron-phonon dynamics dominated by the asymmetry in the carrier distribution, we have observed coherent phonons in p-type Si [2].

We performed time-resolved reflectivity measurements with a sub-10-fs Ti:sapphire oscillator at a center wavelength of 780 nm. Samples were non-doped Si and p-type Si. The carrier concentration in the p-type Si was $3 \times 10^{19} - 1.5 \times 10^{20} / \text{cm}^3$.

The time-resolved reflectivity changes for non-doped Si and the p-type Si are shown in Figs. 1(a) and (b), respectively. The oscillatory signal, originating from coherent phonons in Si, is observed after an overlap between the pump and probe pulses at $t=0$. In the p-type Si, the decay from the photo-generated carriers, which distribute anisotropically in k -space (i.e., anisotropic state-filling), is observed as shown by the dotted line in Fig. 1(b). In the p-type Si, the Fermi level is lowered in the valence band with the non-parabolic structure, which causes the anisotropic hole distribution [2]. When the oscillatory signal is fitted with $\cos(\omega_0 t + \phi)$, where ω_0 and ϕ correspond to the frequency and initial phase of the coherent phonons, respectively, the initial phase in the p-type Si is shifted to the cosine phase with the anisotropy in the hole distribution.

This research was supported by KAKENHI.

- [1] F. Cerdeira, T. A. Fjeldly, and M. Cardona, Phys. Rev. B **8** (1973) 4734.
[2] K. Kato, A. Ishizawa, K. Oguri, K. Tateno, T. Tawara, H. Gotoh, and H. Nakano, Jpn. J. Appl. Phys. **48** (2009) 100205.

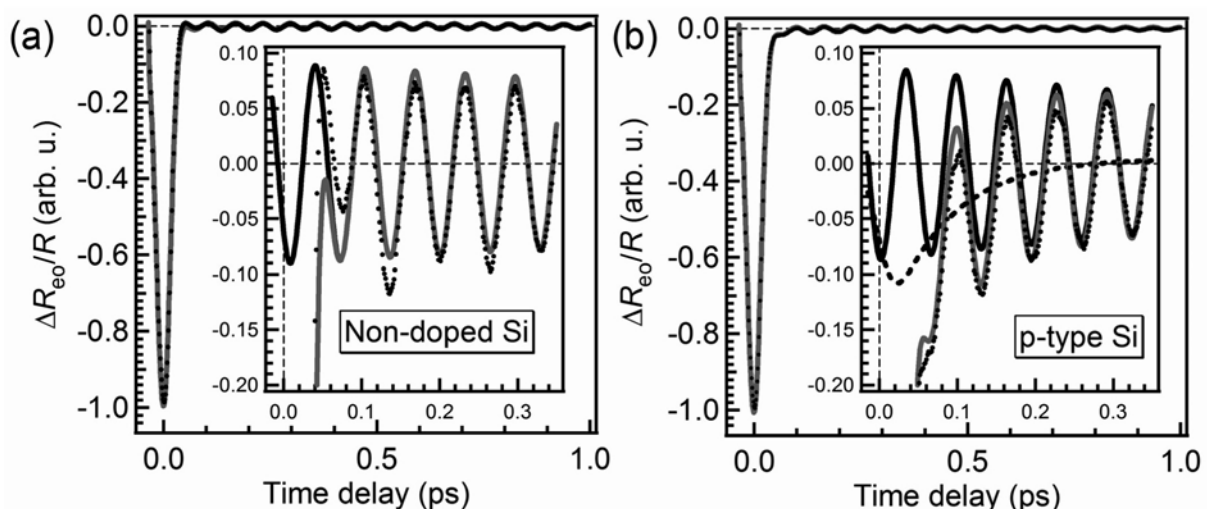


Fig. 1. Time-resolved reflectivity for (a) non-doped Si and (b) the p-type Si. Insets show enlarged graphs around $t=0$. Black dots are the experimental results. The gray line is the fitting result, the black solid line is the component of coherent phonons, and the black dotted line is the decay of anisotropic state-filling.

Freestanding GaAs Nanowires with a Controlled Diameter and Their Optical Properties with the Radial Quantum-confinement Effect

Guoqiang Zhang, Kouta Tateno, Haruki Sanada, and Hideki Gotoh
Optical Science Laboratory

Semiconductor nanowires (NWs) have attracted considerable attention owing to the interesting fundamental properties of such low-dimensional systems and the exciting prospects of utilizing these materials in nanotechnology-enabled electronic and photonic applications. NWs are expected to provide the building blocks with which to form new nanostructures and realize novel 1-dimensional structures. To explore the potentially unique applications of these freestanding NW building blocks, we synthesized freestanding GaAs NWs with a controlled diameter and studied their optical properties with the radial quantum-confinement effect.

The NW growth was undertaken in a metalorganic vapor phase epitaxy system and Au nanoparticles were used to catalyze the NW growth via the vapor-liquid-solid (VLS) mode [1]. We controlled the diameter of the GaAs NWs by using size-selective Au colloidal particles with nominal diameters of 5, 10, 20, 40, and 60 nm [2]. We characterized the structure and diameter of the NWs using transmission electron microscopy (see Fig. 1). We successfully controlled the NWs with very few stacking faults by growing them at a very low temperature. We studied their optical properties by employing micro-photoluminescence (PL) at 3.6 K [3]. Figure 2(a) shows PL spectra from individual NWs of different Au particle sizes. PL peak energies clearly exhibit the blue shift with decreasing Au particle size due to the radial quantum-confinement effect [2]. We analyzed the absorption and emission polarization characteristics of these NWs and found large anisotropies between polarization resolved PL spectra (see Fig. 2(b)). These results suggest that both the dielectric constant contrast and the quantum-confinement effect have to be considered [2]. This work opens the way to investigating size-related optical phenomena in bare GaAs quantum wires, and provides more opportunities for the study of one-dimensional quantum physics using freestanding NWs.

- [1] G. Zhang et al., *J. Appl. Phys.* **103** (2008) 014301.
- [2] G. Zhang et al., *Appl. Phys. Lett.* **95** (2009) 123104.
- [3] G. Zhang et al., *Jpn. J. Appl. Phys.* **49** (2010) 015001.

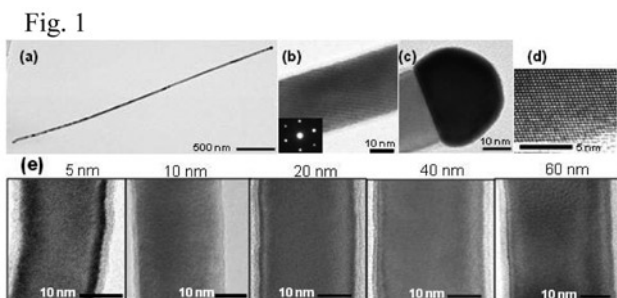


Fig. 1. TEM images of free standing GaAs NWs. (a) Single NW. (b) and (c) high-magnification images of the segments near the middle and tip in (a). The inset in (b) is the corresponding diffraction pattern, which indicates a zinc-blende structure. (d) HRTEM image near the NW side. (e) Images for Au particles with different diameters.

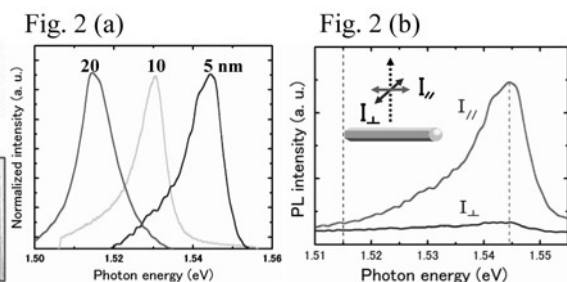


Fig. 2. (a) PL spectra of single GaAs NWs grown using Au particles with three nominal diameters. (b) Polarization resolved PL spectra. The red broken line indicates the free excitonic PL energy in bulk GaAs.

Photoluminescence Properties of Dynamic Quantum Dots Formed by Surface Acoustic Waves

Tetsuomi Sogawa, Haruki Sanada, and Hideki Gotoh
Optical Science Laboratory

Surface acoustic waves (SAWs) provide a dynamic one- or two-dimensional lateral modulation of the band structure of quantum wells (QWs) [1, 2]. In this study, we investigate the dynamic optical properties of excitons in GaAs/AlAs moving dots (dynamic quantum dots, DQDs) formed by the interference of orthogonally propagating SAW beams. The SAWs induce a strain as well as a piezoelectric modulation of the materials properties. Due to the D_{4d} symmetry of the underlying GaAs crystal, the interference of the two orthogonal SAW beams leads to the formation of two interpenetrating square arrays of DQDs [3], as shown in Fig. 1(a), where the in-plane components of the particle displacement field are shown schematically. One of the arrays (black and gray circles) consists of potential dynamic dots (p-DDs) created by the modulation of the piezoelectric potential. The second array (black and gray squares) is composed of strain dynamic dots (s-DDs), where the band gap becomes minimum or maximum due to the modulation of the hydrostatic strain.

Spatially resolved photoluminescence (PL) measurement at 4 K was carried out by using a synchronized excitation method [1]. Figure 1(b) shows the PL mapping for a 6.3-nm QW recorded at a photon energy of 1.623 eV, which is located in the lower-energy side of the PL peak (centered at 1.630 eV in the absence of a SAW). In the PL polarization studies, we define the degree of polarization anisotropy ρ as the relative difference $\rho = (PL_{[1-10]} - PL_{[110]}) / (PL_{[1-10]} + PL_{[110]})$ between the PL intensity emitted along the [1-10] ($PL_{[1-10]}$) and [110] ($PL_{[110]}$) propagation directions of the individual SAW beam. Figures 1 (b) and (c) clearly demonstrate the formation of the two DQD arrays. The strong and weak PL positions in Fig. 1(b) correspond to the tensile (black squares in Fig. 1(a)) and compressive (gray squares in Fig. 1(a)) s-DD positions, respectively. In contrast, the positive (negative) ρ areas in Fig. 1 (c) are located at the saddle point of the tensile (compressive) s-DDs along the [1-10] ([110]) direction, denoted by a black (gray) circle in Figs. 1 (b) and (c). The positions with strong PL anisotropy correspond to the array of the p-DDs.

- [1] T. Sogawa et al., Phys. Rev. B **80** (2009) 075304.
 [2] T. Sogawa et al., Appl. Phys. Lett. **91** (2007) 141917.
 [3] F. Alsina et al., Solid State Commun. **129** (2004) 453.

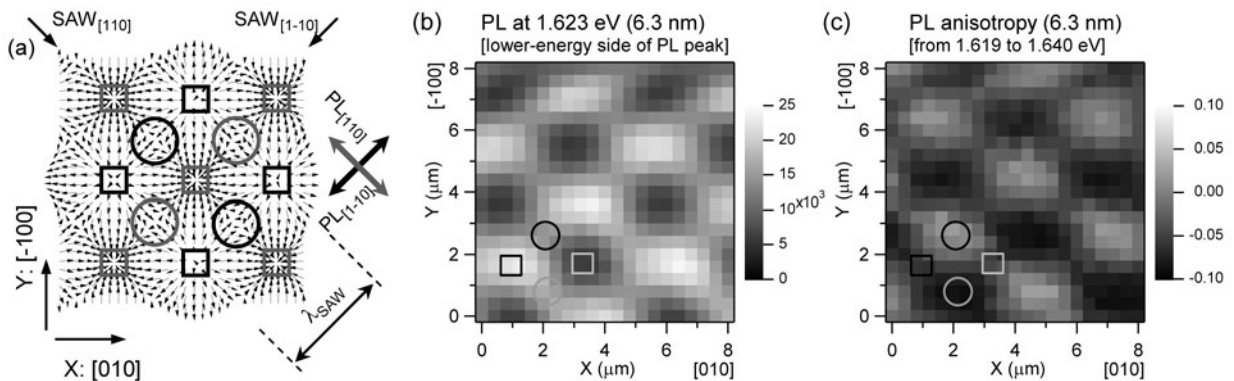


Fig. 1. (a) Schematic illustration of the in-plane components of the particle displacement field. (b) PL mapping for the 6.3-nm QW recorded at a photon energy of 1.623 eV, which is located in the lower-energy side of the PL peak. (c) Spatial distribution of the PL anisotropy for 6.3-nm QW.

Sub-femtojoule All-optical Switching Using a Photonic Crystal Nanocavity

Kengo Nozaki, Takasumi Tanabe, Akihiko Shinya, Shinji Matsuo*, Tomonari Sato*,
Hideaki Taniyama, and Masaya Notomi
Optical Science Laboratory, *NTT Photonics Laboratory

Photonic crystal (PhC) nanocavities, which exhibit a high cavity Q and an ultrasmall modal volume V , allow a strong light-matter interaction. As a result we can expect them to provide the basis for very low power active devices. In particular, the energy needed for all-optical switching based on the carrier-induced resonance shift should be effectively reduced, because the required control energy should be proportional to V/Q . In this study, we successfully achieved an extremely low switching energy and a fast switching time by combining InGaAsP, which exhibits a strong carrier-based nonlinearity, and an ultrasmall PhC nanocavity.

Figure 1(a) and (b) are a top-view image of the PhC structure and the transmission spectrum, respectively. The H0 nanocavity is formed by shifting two adjacent air holes in opposite directions. A computational calculation produced a modal volume V of only $0.025 \mu\text{m}^3$. Figure 2 shows the switching dynamics measured with a pump-probe technique. When the probe pulse wavelength matches the modal peak, the probe pulse transmission is abruptly switched off when the pump pulse temporally overlaps the probe pulse. In contrast, the probe transmission is switched on at shorter probe wavelengths. This is because carrier nonlinearity induces a resonant blueshift. The minimum switching time window of 20 ps is attributed to localized carrier generation and a fast carrier escaping from the cavity. The switching energy with a contrast of 3 dB is only 0.42 fJ, which is more than two orders of magnitude lower than that of previously reported all-optical switches.

We showed that an InGaAsP-PhC nanocavity offers the possibility of realizing an all-optical switch operating with ultrasmall energy, a fast response time, and ultrasmall footprint integratability on a single chip. Other PhC-based optical devices, such as optical memories, photo-detectors, and modulators can also be achieved for chip-scale electronics-photonics interconnection.

This work was partly supported by CREST of Japan Science and Technology Agency.

[1] T. Tanabe et al., Appl. Phys. Lett. **87** (2005) 151112.

[2] K. Nozaki et al., Nature Photon. (in press).

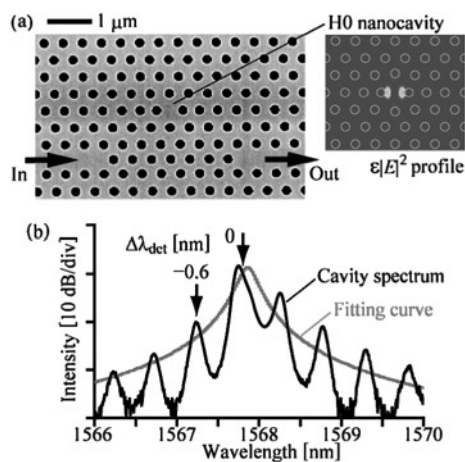


Fig. 1. (a) Top-view image and calculated mode profile of H0 nanocavity. (b) Transmission spectrum with calculated fitting curve.

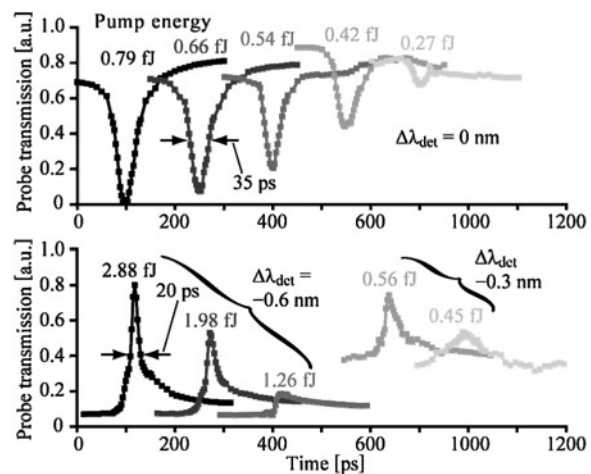


Fig. 2. Switching dynamics. The upper and lower plots are for switch-off and switch-on operations, respectively. $\Delta\lambda_{\text{det}}$ denotes the detuning of a probe wavelength from the modal peak.

Strong Optomechanical Coupling in a Bi-layer Photonic Crystal

Young-Geun Roh, Takasumi Tanabe, Akihiko Shinya, Hideaki Taniyama, Eiichi Kuramochi, Shinji Matsuo*, Tomonari Sato*, and Masaya Notomi
Optical Science Laboratory, *NTT Photonics Laboratories

Mechanical interaction between light and matter is one of the most fundamental problems in physics. Recently, coupling phenomena between optical and mechanical resonant modes in photonic structures has attracted strong interests. In 2006, our group theoretically predicted that a bi-layer photonic crystal (PhC) with a thin air gap can generate strong radiation force [1]. In this work, we have realized a bi-layer PhC for the first time and have demonstrated strong optomechanical coupling in it [2].

A periodic hole pattern arranged in a square lattice was fabricated in two vertically separated slabs using electron beam lithography, dry-wet etching, and CO₂ supercritical drying (Fig. 1). The period, hole diameter, slab thickness, and gap thickness are 750 nm, 540 nm, 200 nm, and 200 nm, respectively. We performed reflectance spectrum measurements of the bi-layer PhC formed in the lateral area of 30×20 μm, which revealed photonic bandedge resonant modes around 1567 nm and 1457 nm. These modes exhibit opposite mode symmetry along the vertical direction. Figure 2 shows reflectance spectra obtained by wavelength scan around symmetric mode (1567 nm), which exhibit input power dependence and optical bistability. We concluded that the observed redshift is explained by a slab displacement (i.e. gap decrease) induced by attractive radiation force for the symmetric resonant mode. The thermo-optically induced shift is excluded because we observed opposite blueshift for the antisymmetric mode (1457 nm). We estimated that each slab was displaced by 0.9 nm at P_{in}=13 mW when the redshift was 1.8 nm. This corresponds to attractive force of 10.8 nN, and thus F/U (i.e. generated force per unit energy in cavity) can be estimated 0.4 μN/pJ, which is a very large value among various optomechanical systems. Thanks to this large optomechanical coupling, we have successfully observed tiny Brownian motion of mechanical modes of bi-layer PhCs [shown in Fig. 3(a)] in RF spectra of the reflected light beam [Fig. 3(b)].

[1] M. Notomi et al., Phys. Rev. Lett. **97** (2006) 023903.

[2] Y. Roh et al., Phys. Rev. B **81** (2010) 121101(R).

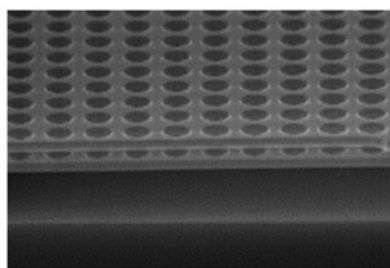


Fig. 1. SEM image of fabricated bi-layer PhC.

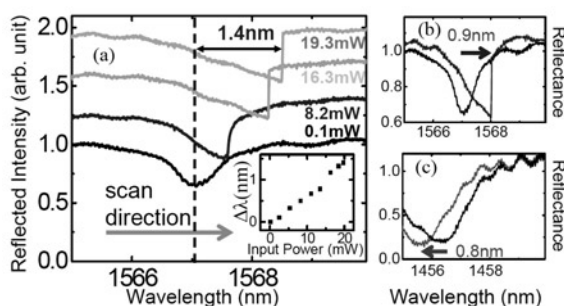


Fig. 2. (a) Power dependence of reflectance spectra.
(b),(c) Simultaneous scan of each resonant mode

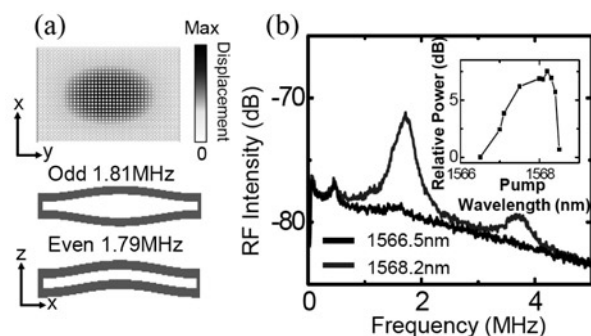


Fig. 3. (a) Fundamental vibration mode of bi-layer PhC. (b) RF spectra of reflected beam

All-silicon Photonic Crystal Receiver for 1.55- μm Light Detection Utilizing Two Photon Absorption

Takasumi Tanabe, Hisashi Sumikura, Hideaki Taniyama, Akihiko Shinya,
and Masaya Notomi
Optical Science Laboratory

Silicon (Si) is widely used to constitute electrical circuits, but it is also a good material for constructing optical integrated circuits. Indeed, optical waveguides and nanocavities have been fabricated on Si chips. However, Si cannot be used to detect 1.5- μm light because it is transparent in this wavelength region. Therefore, germanium (Ge) on Si detectors have been fabricated, but these detectors exhibit a relatively large dark current because of the 4 % lattice mismatch between Ge and Si [1]. In addition, ion-implanted Si detectors have been studied, but they also suffer from a large dark current because of the presence of defects [2]. If we can fabricate an all-Si detector, we should benefit from a low dark current because of the good crystal quality of Si. For this purpose, we need to employ two-photon absorption (TPA) whose coefficient is usually very small. In this study, we used a very high- Q photonic crystal (PhC) nanocavity to compensate for the low TPA coefficient and to enable us to detect very weak optical light in an all-Si device [3].

Figure 1 is an illustration of our pin integrated PhC nanocavity. The Q of the fabricated device was 4.3×10^5 and the transmittance was 24 % [Fig. 2(a) inset]. The dark current was just -15 pA when we applied -3 V bias. Figure 2(a) shows photocurrent versus input power. Due to the strong light confinement of the nanocavity, the TPA current is visible at an extremely low input power of 10^{-8} W. The QE at an input power of 1.17 μW was very high at ~ 10 % (we define QE as 100 % when one photon generates one electron). This value corresponds to 44 % of the cavity-coupled light being sufficiently absorbed. Such a high detection efficiency with 1.55 μm light is obtained because of the high Q of the PhC nanocavity.

We also demonstrated 0.1-Gb/s photo receiver operation using the same device [Fig. 2(b)]. Only light that can resonate with the cavity was detected electrically. This demonstration shows that our Si-chip integrated device can be used for telecom light detection.

[1] S. Assefa, F. Xia, and Y. Vlasov, *Nature* **262** (2010) 80.

[2] M. Geis et al., *Opt. Express* **17** (2009) 5193.

[3] T. Tanabe et al., *Appl. Phys. Lett.* **96** (2010) 101103.

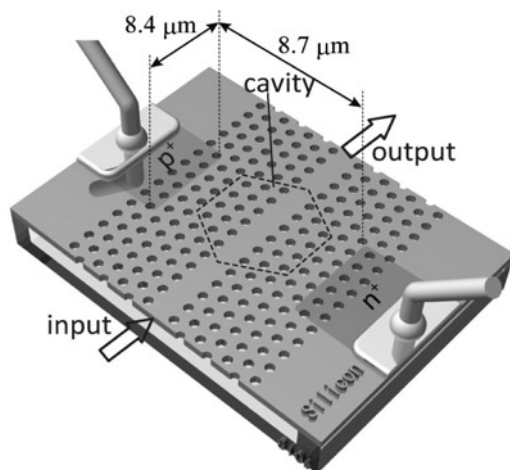


Fig. 1. Schematic illustration of pin integrated photonic crystal nanocavity.

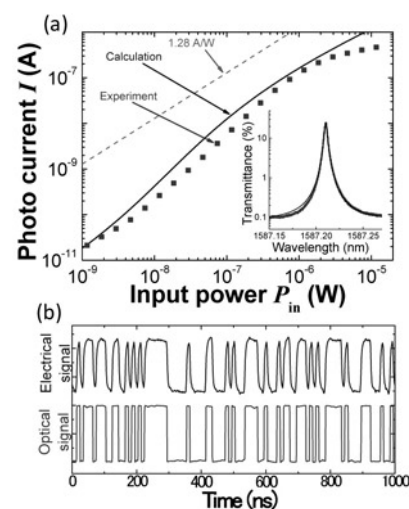


Fig. 2. (a) Input power versus photocurrent. Inset is the transmittance spectrum. (b) 0.1-Gb/s photo receiver demonstration.

II . Data

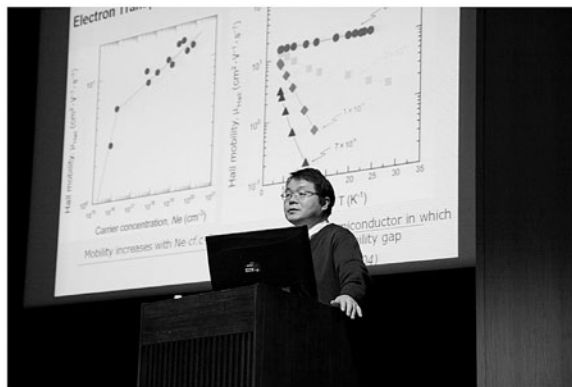
Science Plaza 2009

"Science Plaza 2009," an open-house event of NTT Basic Research Laboratories (BRL), was held at NTT Atsugi R&D Center on Friday, November 27th, 2009. Under the banner "Nanoscience Opens Up the Quantum World", Science Plaza aimed to disseminate our latest research accomplishments through various sections of people inside and outside of NTT and to gather diverse opinions.

Following an opening address from Dr. Itaru Yokohama, the director of BRL, one of distinguished technical members of NTT BRL, Dr. Koji Muraki gave a lecture on "Electron correlation in semiconductor nanostructures — deriving natural team play from electrons-". In the afternoon session, Prof. Hideo Hosono, Tokyo Institute of Technology, gave a special lecture entitled "Real joy of material research — Toward discovery of treasure trove —". Each lecture was well-attended and followed by heated question-and-answer sessions.

As regards the poster exhibits, 44 posters, including 13 from Microsystem Integration Laboratories and Photonics Laboratories, presented our latest research accomplishments. While explaining the originality and impact — as well as the future prospects — of our research accomplishments, these posters were intensively discussed, and many meaningful opinions were heard. This year's "Lab. Tour" — a guided tour of research facilities at NTT BRL that has been receiving high reputation from visitors over the years — took place at five different labs, so that as many people as possible could join the tour. This time we also opened a booth to show the NTT R&D recruitment system for job-seeking researchers and students. After all lectures, presentations, and exhibitions, a banquet was held in Center's dining room, where lively conversation among participants deepened their amity.

More than 220 people from research institutes, universities, and general industries, as well as from NTT Group, attended Science Plaza 2009. Thanks to the efforts of all participants, the conference ended on a high note. We would thus like sincerely to express our gratitude to all of the participants.



5th NTT-BRL School

The fifth NTT Basic Research Laboratories (BRL) school was held from November 24-27, 2009 at the NTT Atsugi R&D Center. The aim of the NTT-BRL school is to foster young researchers in physics and applied physics field and to promote the international visibility of NTT BRL. This year the theme was "Current Research on Cutting-edge Materials", which is closely related to the intensive research based on the materials that NTT BRL is conducting. Prestigious professors and researchers were invited to the school as lecturers. There were thirty-five participants, who were mainly Ph. D students, from nine countries.

On the first day, after the director of NTT BRL had provided an overview of NTT BRL, Prof. Klaus Ploog (Former Director of Paul-Drude-Institute, Germany) presented lectures entitled "Advanced materials for information storage". He also gave lectures every day during the school that covered sustainable energy based on the materials science from the ecological point of view. Prof. Takao Someya (The University of Tokyo, Japan) gave a talk on "Organic materials for electronics, displays, LEDs" on the afternoon of the first day. In this school, there were several lectures by researchers working at NTT BRL. Dr. Toshiki Makimoto gave a lecture on "State-of-the-art Devices using Group-III Nitride Semiconductors". Dr. Hiroshi Yamaguchi talked about the "Micro/nanomechanical Devices using Compound Semiconductor". Dr. Masaya Notomi gave a talk entitled "Perspective on artificial dielectrics". A poster session was held in the evening of the second day, where each student gave a presentation about his/her research at the university. All the students, lecturers, and NTT BRL researchers had a good time exchanging information on current research topics in various fields. On the second and third days we provided an overview of NTT BRL. A laboratory tour was conducted so that the students could see the research facilities. Managers of NTT BRL gave talks on recent activities at each laboratory. On the final day, all the participants attended NTT BRL Science Plaza 2009, which is an exhibition of recent research achievements and activities. They enjoyed detailed discussions with researchers about on-going research topics.

At the farewell party, best poster prizes were awarded to the students who gave noteworthy presentations. The students were able to network and build friendships and exchange contact addresses. NTT BRL will continue to provide these kinds of occasions to support young researchers and help establish human networks in the fields of physics and applied physics.



Award Winners' List (Fiscal 2009)

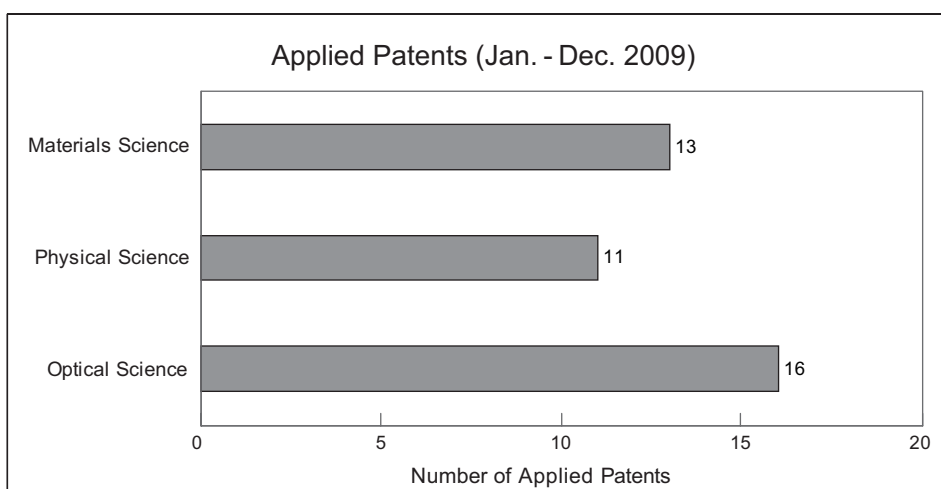
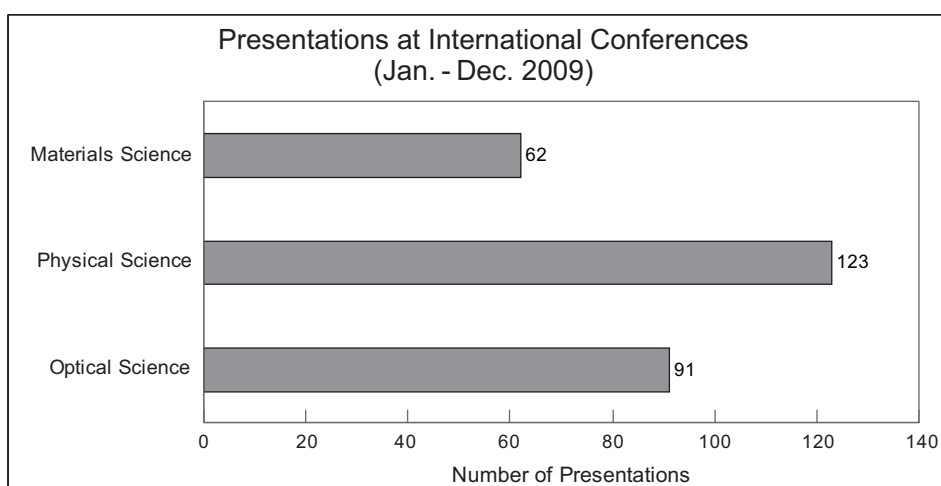
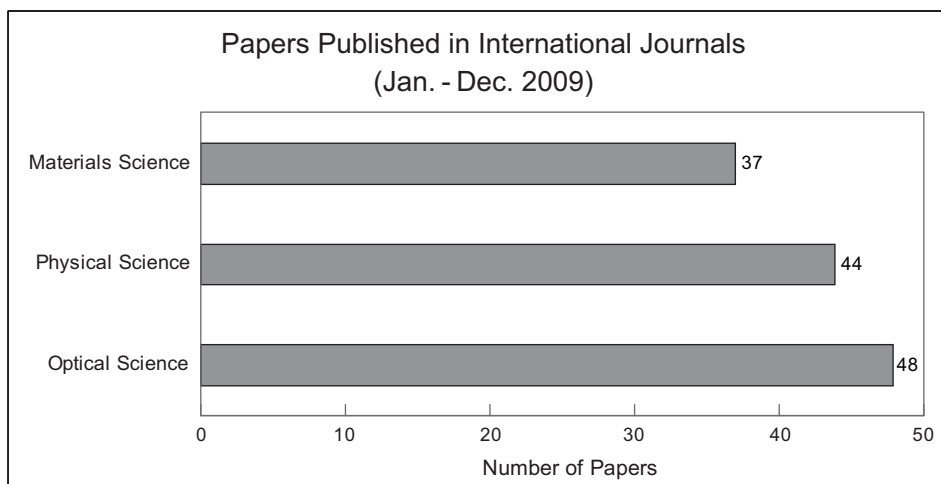
Poster award in International symposium on purinergic signalling in new strategy of drug discovery (Fukuoka Purine 2009)	Y. Shinozaki	Localization of P2X4 receptors in lipid raft-like structure of in vitro model of cell membrane	July. 25, 2009
Japanese Journal of Applied Physics Research Paper Presentation Awards	K. Kakuyanagi	High visibility measurement of superconducting flux qubit using Josephson bifurcation amplifier	Sep. 8, 2009
Certificate of appreciation from The surface science society of Japan	Basic Research Laboratories	Certificate of appreciation	Oct. 28, 2009
3rd International Symposium on Nanomedicine The Best Poster Award	Y. Shinozaki	Direct Visualization of Single Receptor Dynamics: the Relationship between Molecular Scturcture and Physiology/Pathology	Nov. 5, 2009
MNC 2008 Outstanding paper Award	K. Tamaru K. Nonaka M. Nagase H. Yamaguchi S. Warisawa S. Ishihara	Direct actuation of GaAs membrane using microprobe of SPM	Nov. 16, 2009
MNC 2008 Young Authors Award	K. Tamaru	Direct actuation of GaAs membrane using microprobe of SPM	Nov. 16, 2009
Japan Electronic Materials Society, outstanding performance award	H. Wakahara	Observation of exciton and free career electroluminescenece from a carbon nanotube by simultaneous optical and electric measurements	Nov. 20, 2009
Award from Committee of semiconductor interface control	Basic Research Laboratories	Award	Nov. 20, 2009
Iijima Award	D. Takagi	Carbon Nanotube Growth from Diamond Nanoparticles	Mar. 3, 2010

In-house Award Winners' List (Fiscal 2009)

NTT R&D Award	I. Mahboob H. Okamoto K. Onomitsu H. Yamaguchi	"Realization of new functional devices based on semiconductor mechanical resonators"	Dec. 9, 2009
NTT R&D Award	M. Yamaguchi K. Suzuki Y. Ono	"Great improvement of recovery rate of liquid helium and reduction in fixed costs by introduction of a new management system"	Dec. 9, 2009
Award for Achievements by Director of Basic Research Laboratories	T. Fujisawa G. Shinkai T. Hayashi T. Ota	"Development of multi-functional quantum information processing devices using two-qubit structures"	Mar. 26, 2010
Award for Achievements by Director of Basic Research Laboratories	Y. Shinozaki N. Kasai K. Sumitomo K. Torimitsu	AFM study of structure and dynamics in a membrane receptor protein	Mar. 26, 2010
Award for Achievements by Director of Basic Research Laboratories	D. Takagi Y. Kobayashi	"Development of new catalysts for carbon nanotube growth"	Mar. 26, 2010
Award for Excellent papers by Director of Basic Research Laboratories	T. Tanabe M. Notomi H. Taniyama E. Kuramochi	"Dynamic Release of Trapped Light from an Ultrahigh-Q Nanocavity via Adiabatic Frequency Tuning", <i>Phys. Rev. Lett.</i> 102 (2009) 043907.	Mar. 26, 2010
Award for Excellent papers by Director of Basic Research Laboratories	H. Hibino H. Kageshima M. Nagase Y. Kobayashi H. Yamaguchi	"Microscopic thickness determination of thin graphite films formed on SiC from quantized oscillation in reflectivity of low-energy electrons", <i>Phys. Rev. B</i> 77 (2008) 075413.	Mar. 26, 2010
Award for Excellent papers by Director of Basic Research Laboratories	K. Tamaki	"Unconditional security of the Bennett 1992 quantum-key-distribution scheme with a strong reference pulse", <i>Phys. Rev. A</i> 80 (2009) 032302.	Mar. 26, 2010
Award for encouragement by Director of Basic Research Laboratories	H. Okamoto	"Optical control of mechanical vibration in nanomechanical resonators"	Mar. 26, 2010

Research Activities in Basic Research Laboratories in 2009

The numbers of papers published in international journals, presentations at international conferences and applied patents in year 2009 amounted to 129, 276, and 40, respectively. The numbers for each research area are as follows;



The numbers of research papers published in the major journals are shown below.

Journals	(IF2008*)	Numbers
Applied Physics Letters	3.726	11
Physical Review B	3.322	11
Applied Physics Express	-	9
Japanese Journal of Applied Physics	1.309	9
Optics Express	3.88	9
Physical Review Letters	7.18	8
Physical Review A	2.908	7
International Journal of Modern Physics B	0.558	5
Nanotechnology	3.446	4
Journal of the American Chemical Society	8.091	1
The Journal of Physical Chemistry B	4.189	1
Nature Physics	16.821	1
PLoS Biology	12.683	1
Reports on Progress in Physics	12.09	1
Small	6.525	1

*IF2008: Impact Factor 2008 (Journal Citation Reports,2008)

The average IF2008 for all research papers from NTT Basic Research laboratories is 3.58.

The numbers of presentations in the major conferences are shown below.

Conferences	Numbers
International Symposium on. Nanoscale Transport and Technology 2009	42
The 18th International Conference on Electronic Properties of Two-Dimensional Systems	24
2009 International Conference on Solid State Devices and Materials	17
29th Conference on Lasers and Electro Optics and the 27th International Quantum Electronics Conference	9
The 12th International Superconductive Electronics Conference	7
International Symposium on Advanced Nanodevices and Nanotechnology	6
14th Narrow Gap Semiconductor and Systems	6
14th International Conference on Modulated Semiconductor Structures	6
22nd International Microprocesses and Nanotechnology Conference	6
Materials Research Society Meeting	5
The European Conference on Lasers and Electro-Optics and the XIth European Quantum Electronics Conference	4
2009 American Physical Society March Meeting	4
Neuroscience 2009	4
13th International Conference on Silicon Carbide and Related Materials	4
Silicon Nanoelectronics Workshop	4
International Symposium on Nanomedicine	4
17th International Colloquium on Scanning Probe Microscopy	4
Asia-Pacific Workshop on Fundamental and Application of Advanced Semiconductor Devices	3
8th International Conference on Nitride Semiconductor	3
The 22nd Annual Meeting of the IEEE Photonics Society	3
International Union of Physiological Science 2009	3
SPIE Photonics West 2009	3
International Symposium on Nanoscience and Quantum Physics 2009	3
The 9th International Conference on Materials and Mechanisms of Superconductivity	3
Emergent Phenomena in Quantum Hall Systems 3	3
The 9th European Conference on Applied Superconductivity	3
The 36th International Symposium on Compound Semiconductors	3

List of Invited Talks at International Conferences (2009)

I. Materials Science Laboratory

- (1) H. Omi, H. Kageshima, S. Uematsu, T. Kawamura, Y. Kobayashi, S. Fujikawa, Y. Tsusaka, Y. Kagoshima, and J. Matsui, "Stability-instability transition of reaction fronts in thermal silicon oxidation", Symposium on Surface and Nano Science 2009, Shizukuishi, Japan (Jan. 2009).
- (2) Y. Taniyasu and M. Kasu, "Recent progress in AlN deep-UV light-emitting diodes: physics and device structure", SPIE Photonics West, San Jose, U.S.A. (Jan. 2009).
- (3) M. Kasu, "Nitride semiconductors and diamond", Ambient GCOE Research Exchange Seminar, "Wide Gap Semiconductor; the presence and its future" Waseda Univ, Japan. (Mar. 2009).
- (4) M. Kasu, K. Ueda, Y. Taniyasu, and K. Michal, "Progress of diamond semiconductor technologies: doping and heterostructures", 3rd Industrial Diamond Conference, Paris, France (Apr. 2009).
- (5) H. Omi, T. Kawamura, and Y. Kobayashi, "Advanced SOI interface characterization using grazing incidence X-ray diffraction", 215th The Electrochemical Society Meeting, San Francisco, U.S.A. (May 2009).
- (6) D. Takagi, Y. Kobayashi, and Y. Homma, "Single-walled carbon nanotube growth from nanosized diamond particles by chemical vapor deposition", New Diamond and Nano Carbons Conference 2009, Traverse City, Michigan, U.S.A. (June 2009)
- (7) S. Suzuki and Y. Kobayashi, "Defect engineering in single-walled carbon nanotubes", 25th International Conference on Defects in Semiconductors, St.Petersburg, Russia (July 2009).
- (8) K. Torimitsu, "Effect of Mg²⁺ on rat neural activity in vitro", 12th International Magnesium Symposium, Lasi, Romania (Sep. 2009).
- (9) H. Hibino, H. Kageshima, and M. Nagase, "Structure and electronic properties of epitaxial graphene grown on SiC studied by surface electron microscopy", 22nd International Microprocesses and Nanotechnology Conference, Sapporo, Japan (Nov. 2009).
- (10) K. Furukawa, "Supported lipid bilayer formation at interface", International Symposium on Nanomedicine, Okazaki, Japan (Nov. 2009).
- (11) M. Kasu, "Ultimate widegap semiconductors: diamond and aluminum nitride", Joint NTUU "KPI" and NTT seminar, Kiev, Ukraine (Nov. 2009).
- (12) K. Torimitsu, "Understanding receptor protein structure and functions for biomimetic device", 3rd International Symposium on Nanomedicine, Okazaki, Japan (Nov. 2009).
- (13) H. Hibino, H. Kageshima, and M. Nagase, "Microscopic evaluations of structure and electronic properties of epitaxial graphene", 7th International Symposium on Atomic Level Characterizations for New Materials and Devices, Hawaii, U.S.A. (Dec. 2009).

II. Physical Science Laboratory

- (1) K. Muraki, "Spin-dependent phase diagram in bilayer 2D electron systems", APS March Meeting 2010, Oregon, U.S.A. (Mar. 2009).
- (2) M. Nagase, H. Hibino, H. Kageshima, and H. Yamaguchi, "Novel microscopies for graphene on SiC", 2009 RCIQE (Research Center for Integrated Quantum Electronics) International Seminar, Sapporo, Japan (Mar. 2009).
- (3) H. Yamaguchi, "Micro/Nanomechanical systems based on compound semiconductor heterostructures", Frontiers in Nanoscale Science and Technology 2009 (FNST 2009), Boston, U.S.A (May 2009).
- (4) K. Muraki, "New lights on the ground-state phase diagrams of bilayer electron systems", Emergent Phenomena in Quantum Hall Systems 3 (EPQHS-3), Capannori (Lucca), Italy (Jun. 2009).
- (5) M. Nagase, H. Hibino, H. Kageshima, and H. Yamaguchi, "Metrology of microscopic properties of graphene on SiC", 2009 Asia-Pacific Workshop on Fundamentals and Applications of Advanced Semiconductor Devices, Busan, Korea (Jun. 2009).
- (6) H. Yamaguchi, "Heterostructure-based micro/nanomechanical systems", The 18th International Conference on Electronic Properties of Two-Dimensional Systems (EP2DS), Kobe, Japan (Jul. 2009).
- (7) K. Semba, J. Johansson, K. Kakuyanagi, H. Nakano, S. Saito, H. Tanaka, and H. Takayanagi, "Quantum state control, entanglement, and readout of the Josephson persistent current qubit", Solid State Based Quantum Information Processing 2009 (QIP 2009), München, Germany, (Jul. 2009).
- (8) H. Yamaguchi, "Compound semiconductor micro/nanomechanical systems", 8th Topical Workshop on Heterostructure Microelectronics (TWHM2009), Nagano, Japan (Aug. 2009).
- (9) A. Fujiwara, K. Nishiguchi, and Y. Ono, "Single-electron devices based on silicon nanowire MOSFETs", 10th Trends in Nanotechnology International Conference (TNT 2009), Barcelona, Spain, (Sep. 2009).
- (10) A. Fujiwara, K. Nishiguchi, and Y. Ono, "Silicon nanowire MOSFETs and their application to single-electron device", International Conference on Nanoscience and Technology, China 2009 (ChinaNANO 2009), Beijing, China (Sep. 2009).
- (11) Y. Ono, M. Khalafalla, S. Horiguchi, K. Nishiguchi, and A. Fujiwara, "Identification of single boron acceptors in nanowire MOSFETs", 2009 International Conference on Solid State Devices and Materials (SSDM 2009), Sendai, Japan (Oct. 2009).
- (12) I. Mahboob and H. Yamaguchi, "Electromechanical systems for memory and logic devices", 2009 International Conference on Solid State Devices and Materials (SSDM 2009). Sendai, Japan, (Oct. 2009).
- (13) H. Kageshima, H. Hibino, and M. Nagase, "Epitaxial graphene growth using LEEM and first-principles", 13th International Conference on Silicon Carbide and Related Materials (ICSCRM 2009), Nürnberg, Germany, (Oct. 2009).
- (14) K. Semba, "Control of entanglement and quantum superposition of superconducting persistent current qubit few photon system", 22nd International Symposium on Superconductivity 2009 (ISS 2009), Tsukuba, Japan, (Nov. 2009).
- (15) K. Semba, "Superconducting qubit as an entanglement generator", Quantum Technologies: Information and Communication (QTIC 2009), Tokyo, Japan (Dec. 2009).

- (16) M. Nagase, H. Hibino, H. Kageshima, and H. Yamaguchi, "Microscopic characterization of few-layer graphene on SiC", International Symposium on Advanced Nanodevices and Nanotechnology (ISANN 2009), Hawaii, U.S.A. (Dec. 2009).
- (17) M. Nagase, H. Hibino, H. Kageshima, and H. Yamaguchi, "Microscopic characterization of few-layer graphene on SiC using an integrated nanogap probe", 17th International Colloquium on Scanning Probe Microscopy (ICSPM 17), Izu, Japan (Dec. 2009).

III. Optical Science Laboratory

- (1) M. Notomi, "Manipulating light by ultrahigh-Q nanocavities", Nanomata 2009, Tirol, Austria (Jan. 2009).
- (2) T. Tanabe, A. Shinya, E. Kuramochi, H. Taniyama, and M. Notomi, "All-optical switches and bistable devices using high-Q photonic crystal nanocavities", SPIE Photonics West 2009, San Jose, U.S.A. (Jan. 2009).
- (3) M. Notomi, "Evolution of modulated mode-gap cavities", SPIE Photonics West 2009, San Jose, U.S.A. (Jan. 2009).
- (4) K. Tateno, Q. Zhang, and H. Nakano, "Heterostructures in GaP-based free-standing nanowires on Si substrates", SPIE Photonics West 2009, San Jose, U.S.A. (Jan. 2009).
- (5) H. Nakano, A. Ishizawa, and K. Oguri, "Dependence of harmonics generation properties on carrier-envelope phase of few-cycle laser field", COAST/CORAL Symposium on Ultrafast Intense Laser Science, Karuizawa, Japan (Mar. 2009).
- (6) H. Takesue, "Telecom-band entanglement swapping using high-speed singlephoton detectors based on sinusoidally-gated InGaAs/InP avalanche photodiodes", SPIE Defence, Security + Sensing 2009, Advanced Photon Counting Techniques III, Orland, U.S.A. (Apr. 2009).
- (7) M. Notomi, "Strong light confinement with and without periodicity", The 8th International Photonic and Electromagnetic Crystal Structures Meeting (PECS-VIII), Sydney, Australia (Apr. 2009).
- (8) H. Takesue, K. Harada, H. Fukuda, T. Tsuchizawa, T. Watanabe, K. Yamada, Y. Tokura, and S. Itabashi, "Silicon photonics in quantum communications", The Conference on Lasers and Electro-Optics and The Quantum Electronics and Laser Science Conference (CLEO/QELS), Baltimore, U.S.A. (May 2009).
- (9) M. Notomi, "Adiabatic frequency tuning of ultrahigh-Q nanocavities", The 8th International Symposium on Electrical Transport and Optical Properties of Inhomogeneous Media, Crete, Greek (Jun. 2009).
- (10) T. Honjo, A. Uchida, K. Amano, K. Hirano, H. Someya, H. Okumura, K. Yoshimura, P. Davis, and Y. Tokura, "Differential-phase-shift quantum key distribution experiment using fast physical random bit generator with chaotic semiconductor lasers", 18th International Laser Physics Workshop, Barcelona, Spain (Jul. 2009).
- (11) T. Tanabe, M. Notomi, H. Taniyama, and E. Kuramochi, "Recent progress of dynamically tuned photonic crystal nanocavities", 18th International Laser Physics Workshop, Barcelona, Spain (Jul. 2009).
- (12) M. Yamashita, M. W. Jack, K. Inaba, K. Igeta, and Y. Tokura, "Gutzwiller study of Bose-Fermi mixtures trapped in three-dimensional optical lattices", 18th International Laser Physics Workshop, Barcelona, Spain (Jul. 2009).
- (13) M. Notomi, E. Kuramochi, and T. Tanabe, "Manipulating slow light by ultrahigh-Q nanocavities and their coupled arrays", OSA Topical Meeting on Slow and Fast Light 2009, Honolulu, U.S.A. (Jul. 2009).

- (14) K. Tawara, S. Hughes, and H. Kamata, "Cavity mode emission in weakly coupled quantum-dot-cavity system: Photon statistics and mode attraction", Photons and Spins in Nanostructures, Sapporo, Japan (Jul. 2009).
- (15) M. Yamashita, A. Yamamoto, and N. Kawakami, "DMRG study of ultracold fermionic atoms in optical lattices", Workshop on Matrix Product State Formulation and Density Matrix Renormalization Group Simulations, Kobe, Japan (Aug. 2009).
- (16) H. Taniyama, E. Kuramochi, and T. Tanabe, Y-G. Roh, M. Notomi, "High-Q air-slot photonic crystal cavities", 9th International Conference on Numerical Simulation of Optoelectronic Devices, Gwangju, Korea (Sep. 2009).
- (17) A. Shinya, S. Matsuo, K. Nozaki, T. Tanabe, E. Kuramochi, T. Satou, T. Kakitsuka, and M. Notomi, "All-optical memories based on photonic crystal nanocavities", Photonics in Switching 2009, Pisa, Italy (Sep. 2009).
- (18) M. Notomi, E. Kuramochi, T. Tanabe, and H. Taniyama, "Manipulating slow light by ultrahigh-Q nanocavities and their coupled arrays", Frontiers in Optics 2009, San Jose, U.S.A. (Oct. 2009).
- (19) H. Nakano, K. Oguri, Y. Okano, and T. Nishikawa, "Dynamics of femtosecond-laser-ablated liquid-aluminium nanoparticles probed by means of spatiotemporally resolved X-ray-absorption fine-structure spectroscopy", 10th International Conference on Laser Ablation, Singapore, Singapore (Nov. 2009).
- (20) H. Takesue, "Quantum communication experiments using telecom-band entangled photons", International Conference on Quantum Information and Technology (ICQIT), Tokyo, Japan (Dec. 2009).
- (21) H. Nakano, K. Oguri, and A. Ishizawa, "High-order harmonics of carrier-envelope phase controlled few-cycle laser pulse for time-resolved spectroscopy", 5th Asian Symposium on Intense Laser Science, Hanoi, Vietnam (Dec. 2009).
- (22) M. Notomi, "Manipulation of light by photonic crystals", International Conference on Quantum Information and Technologies, Tokyo, Japan (Dec. 2009).

**Research Activities in NTT-BRL
Editorial Committee**

NTT Basic Research Laboratories

3-1 Morinosato Wakamiya, Atsugi

Kanagawa, 243-0198 Japan

URL: <http://www.brl.ntt.co.jp/>